An-Najah National University

Faculty of Graduate Studies

THERMO-OXIDATIVE DECOMPOSITION ANALYSIS OF LEVOFLOXACIN BY ISOCONVERSIONAL KINETICS AND COMPUTATIONAL METHODS

By

"Mohammed Nash'at" Ahmad Thaher

Supervisor

Dr. Ismail Badran

This Thesis is Submitted in Partial Fulfillment of the Requirements for The Degree of Master of Chemistry, Faculty of Graduate Studies, An Najah National University, Nablus-Palestine.

2024

THERMO-OXIDATIVE DECOMPOSITION ANALYSIS OF LEVOFLOXACIN BY ISOCONVERSIONAL KINETICS AND COMPUTATIONAL METHODS

By
"Mohammed Nash'at" Ahmad Thaher

This thesis was Defended successfully on 11/03/2024, and approved by:

Dr. Ismail Badran	Ismail Badran
Supervisor	Signature
Dr. Mohamed Abdelnaby	Mohamed Youssry
External Examiner	Signature
Dr. Amjad El-Qanni	A.E. 15/05/2024
Internal Examiner	Signature

Dedication

I am proud to dedicate this work to my exquisitely caring mother, my tenaciously wise father, and my resilient siblings who stood by my side through thick and thin.

I would also like to dedicate this work to the friends and family members that held me up through tough times.

With all the gratitude and respect in the world.

Acknowledgement

I would like to thank the Department of Chemistry at An-Najah University for assisting in completing this thesis, through their continuous guidance, and their unconditional support. Especially Dr. Ismail Badran, who diligently supervised this work, Dr. Ahed Zyoud, the former head of the Chemistry Department, Dr. Derar Smadi, the current head of Chemistry Department, and Mr. Ameed Amira, the head lab technician at the Chemistry Department laboratories, for their assistance in making this work possible.

Special gratitude to the High-Performance Computing (HPC) facility at An-Najah University for providing the equipment to conduct the Theoretical part of this work. Especially Mr. Mohammad Adas, for his role in cooperation on the technical side of running the facility.

A huge token of gratitude goes out to the University of Jordan for assisting the experimental analysis.

Declaration

I, the undersigned, declare that I submitted the thesis entitled:

THERMO-OXIDATIVE DECOMPOSITION ANALYSIS OF LEVOFLOXACIN BY ISOCONVERSIONAL KINETICS AND COMPUTATIONAL METHODS

Unless otherwise referenced, I declare that the work provided in this thesis is the researcher's work and has not been submitted elsewhere for any other degree or qualification.

Student's Name: محمد نذير أحمد إبراهيم

Signature:

Date: ٢٠٢٤/٣/١١

List of Contents

List of Tables

List of Figures

List of Appendixes

THERMO-OXIDATIVE DECOMPOSITION ANALYSIS OF LEVOFLOXACIN BY ISOCONVERSIONAL KINETICS AND COMPUTATIONAL METHODS

By
"Mohammed Nash'at" Ahmad Thaher
Supervisor
Dr. Ismail Badran

Abstract

This study presents a thorough thermogravimetric analysis (TGA) to comprehend the thermal decompaction of the antibiotic drug levofloxacin, as a model pharmaceutical pollutant. The reaction was analyzed under N_2 gas flow using a TGA analyzer at different heating rates. The isoconversional methods of Kissinger–Akahira–Sunose (KAS) and Friedman were applied to obtain the effective activation energy (E_α) of the decomposition as a function of the extent of conversion (α). The E_α of levofloxacin's decomposition reaction was found to be between 23.3 – 68.5 kJ/mol for the KAS method, and between 48.3 – 117.5 kJ/mol for the Friedman method, positively correlating to α.

Additionally, Differential scanning calorimetry (DSC) was used to assess the thermodynamic physical and chemical changes that occur as a function of temperature. And Density functional theory (DFT) calculations were used to calculate the bond dissociation energies (BDEs) of the levofloxacin possible degradation routes.

The DFT analysis along with DSC and Friedman method's results suggest that the most probable dissociation route is aromatic-Me bond to give off $\bullet CH_3$ radicals.

Keywords, Pharmaceutical. Thermogravimetric analysis. Differential Scanning Calorimetry. Isoconversional. Computational chemistry. Adsorption.

Chapter One

Introduction and Theoretical Background

The bonds hold a molecule of a chemical compound together are a result of an attraction between the nuclei of atoms and the electrons of other atoms by the electromagnetic force. These interactions dictate physical properties for chemical compounds; hence their study is called physical chemistry. These properties include thermodynamic and kinetic effects, of which each require certain experimentation to evaluate, and each serve the understanding of a different parameter about a substance's behavior in conditions that the experiment applies to (1–3).

A combination of these properties provides an understanding of how a certain molecule's bonds behave in interactions with more complex media, such as in a chemical reaction, or a physical interaction. By partitioning these interactions into their most basic formulas it becomes possible to effectively understand the main ways that a molecule interacts with these media, by studying each part of these smaller segments and building a model for the said interaction to take place.

Researchers in the field of thermochemical and kinetic analysis have studied several compounds to determine their mechanism of action in human bodies, decomposition mechanism in the environment or packaging media, reactivity to other drugs, or reactivity to the environment and its individual components. The methods of quantitative and qualitative analysis used widely vary, while their simplicity and accuracy are generally inversely correlated. Therefore, the method used must give the most accurate result while not being too cumbersome as to drain resources in an unnecessary manner. (3, 4)

The excessive use of antibiotics and pharmaceuticals has exacerbated the presence of pollutants in water, posing significant threats to human health. This issue remains a top priority for researchers and environmentalists. Implementing effective removal methods is crucial for fostering a healthier environment, supporting agriculture, and ensuring ecological sustainability (5–7).

Over the last decade, water samples from different sources around the world have been shown to contain contaminants from pharmaceutical and personal care products (PPCPs) (5, 8–10).The sources of this contamination are human excretion, manufacturing waste,

and also the conventional methods of wastewater treatment used in wastewater treatment plants (WWTPs) (6, 9). Literature has hinted at the fact that WWTPs are, therefore, neither well-equipped, nor well-designed, enough to remove PPCPs from wastewater (6, 9).

For this work kinetic analysis experiments will be run on a drug by the name levofloxacin, which is an antibiotic. This drug was chosen for being common in pharmaceutical production, and possesses nitrogen atoms at which the decomposition may lead to the release of molecules that may be then turned into fuel.

This study, is an analysis using isoconversional kinetics and computational chemical calculations, of which the main objective is to explore the thermal decomposition of levofloxacin and define the main pathways of its decomposition.

1.1 Levofloxacin

Levofloxacin, Figures 1 and 2, is a chiral fluoroquinolone antibiotic, that is used to treat a wide range of bacterial infections (11). It is a yellowish-white crystal, and is the pure (-)-(S)-enantiomer of the racemic mixture found in the drug ofloxacin. The systematic name of the drug is "(-)-(S)-9-fluoro-2,3-dihydro-3-methyl-10-(4-methyl1-piperazinyl)-7-oxo-7H-pyrido[1,2,3-de]-1,4-benzoxazine-6-carboxylic acid hemihydrate" (12). The drug is a hemihydrate in the oral form of the medicine, however the crystal is subject to polymorphism when ground, heated and/or treated with different solvents, and produces three different crystal structures (13, 14).

In general quinolones, and specifically fluoroquinolones, work by inhibiting two enzymes involved in the replication of bacterial deoxyribonucleic acid (DNA). These enzymes work to separate and insert DNA strands and rebind them after the replication process ends. Both of these enzymes are topoisomerases that are not found in human cells. Which in turn makes the antibiotic drugs targeted towards bacterial infections and not harmful to a patient's cells. Increasing the effectiveness and reducing the side-effects of such drugs (15).

It was estimated that in 2015 the defined daily dose (DDD) of antibiotics consumed globally were about 42 billion, and at the time the trends showed an increase in consumption projections for low and middle-income countries' consumption rates (16).

The wide consumption of antibiotics, and their tendency to persist in the environment, specifically through wastewater present the need for understanding the drug's waste, and the development of ways for treatment of this waste. Since allergic reactions may be caused to people who are exposed to such waste, along with the risk of endocrine disruption, cancer, and reproductive dysfunctions (4, 17). In addition, the waste from antibiotics generally causes some species of microorganisms to gain immunity to the drug (16, 17), and therefore aid in the creation of what have been referred to as "Superbugs" (18).

Figure 1

Levofloxacin molecule chemical structure (2 Dimensional), where the labels for the atoms were produced by the Avogadro software's internal algorithm

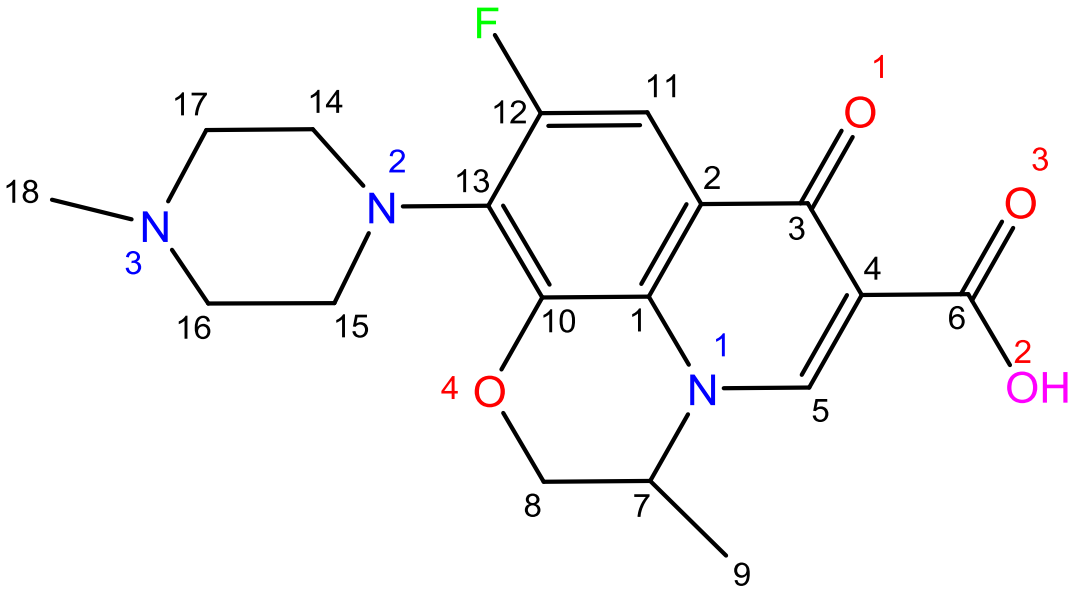

Figure 2

Levofloxacin molecule chemical structure (3 dimensional), where the labels for the atoms were produced by the Avogadro software's internal algorithm

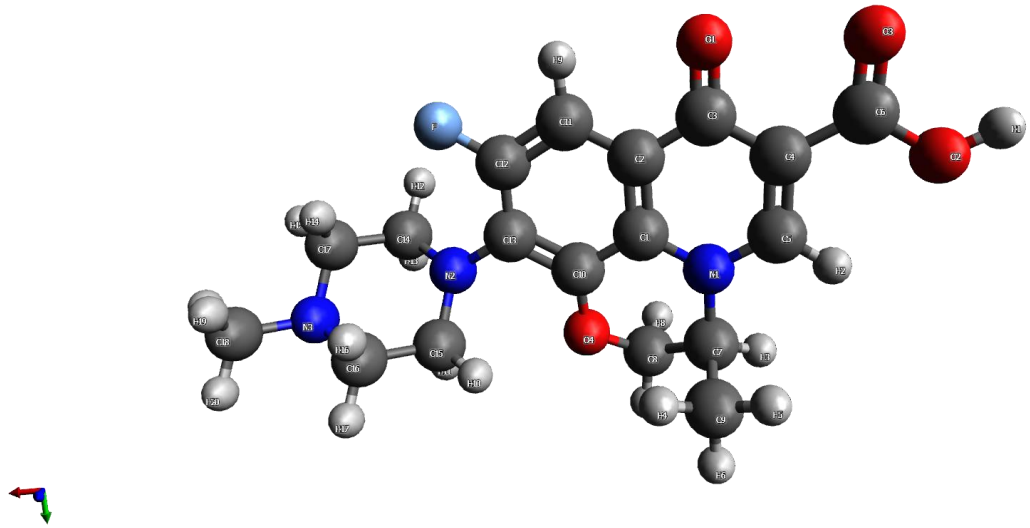

The effects of levofloxacin on the environment have been analyzed by Zhou et al. (19) to be linked to inevitable water pollution, which affects aquatic microorganisms in a significant manner, especially cyanobacteria, with an even greater effect to the cyanobacteria than oxytetracycline that was studied alongside it. While their work also hints at the significance of the possible spread of antibiotic resistance genes in the aquatic environment, which is linked to many environmental risks.

Levofloxacin was mentioned in several studies, some of which studied its chemical properties, such as stereochemistry, in the work of Pereira et al. (13) who found the drug to be susceptible to polymorphism. With three possible crystal structures. Their work suggests that the flow of energy might cause denaturing of the bonds, causing a complex mechanism to emerge of the several outcomes for each pathway of the reaction. Others studied the physical properties, such as Nisar et al. (20) who looked into the effect of thermochemical changes on the drug's properties in light of levofloxacin-excipient interaction, through (TGA) and (DSC) using one of the isoconversional methods, and found that the Eα of levofloxacin was 118 kJ/mol. However, that work did not provide a computational model to compare it to. Whereas, this work, looks into the chemical and physical changes that occur during the decomposition of levofloxacin through different estimations of the effective activation energy using isoconversional kinetics and

computational calculation models. This work builds on the efforts by Badran et al. (4, 17, 21, 9) to find a mechanism to treat pharmaceutical waste.

1.2 Thermochemical analysis

A thermal analysis consists of experimental evaluations that aim to understand the chemical and physical properties of a certain substance. This is done by changing the thermal conditions around the substance, while measuring any physical, or chemical property that the experimentation apparatus is sensitive towards. Therefore, evaluating the effect and the scale of change on the substance provided by that change.

The thermal analysis of this anti-biotic drug gives an idea of the reaction pathdays, to prevent unwanted harm to the environment caused when it is introduced to the environment as waste, and through the manufacturing process (4).

The main focus of this analysis will be on the thermal stability and the drug's chemical behavior at high temperatures. Through the use of thermo-gravimetric analysis (TGA), and differential scanning calorimetry (DSC). These techniques provide a clear demonstration of the behavior of the molecule relative to a change in temperature, which in turn enables the calculation of the energy within the system and how the molecule changes based on the changes in energy input (2, 4, 17, 21, 9).

TGA is conducted using a machine bearing the same name that consists of three compartments, a sample cell, a sensitive balance, and a furnace chamber. A sample is placed in the given cell, that sits atop the scaling balance, the furnace is then lowered into place and the process of heating the sample while at the same time calculating its mass is measured by a computer unit attached to the device. The results are then graphed based on the readings. Figure 3 shows a schematic diagram of the TGA device (22).

Figure 3

Schematic interpretation of a TGA device

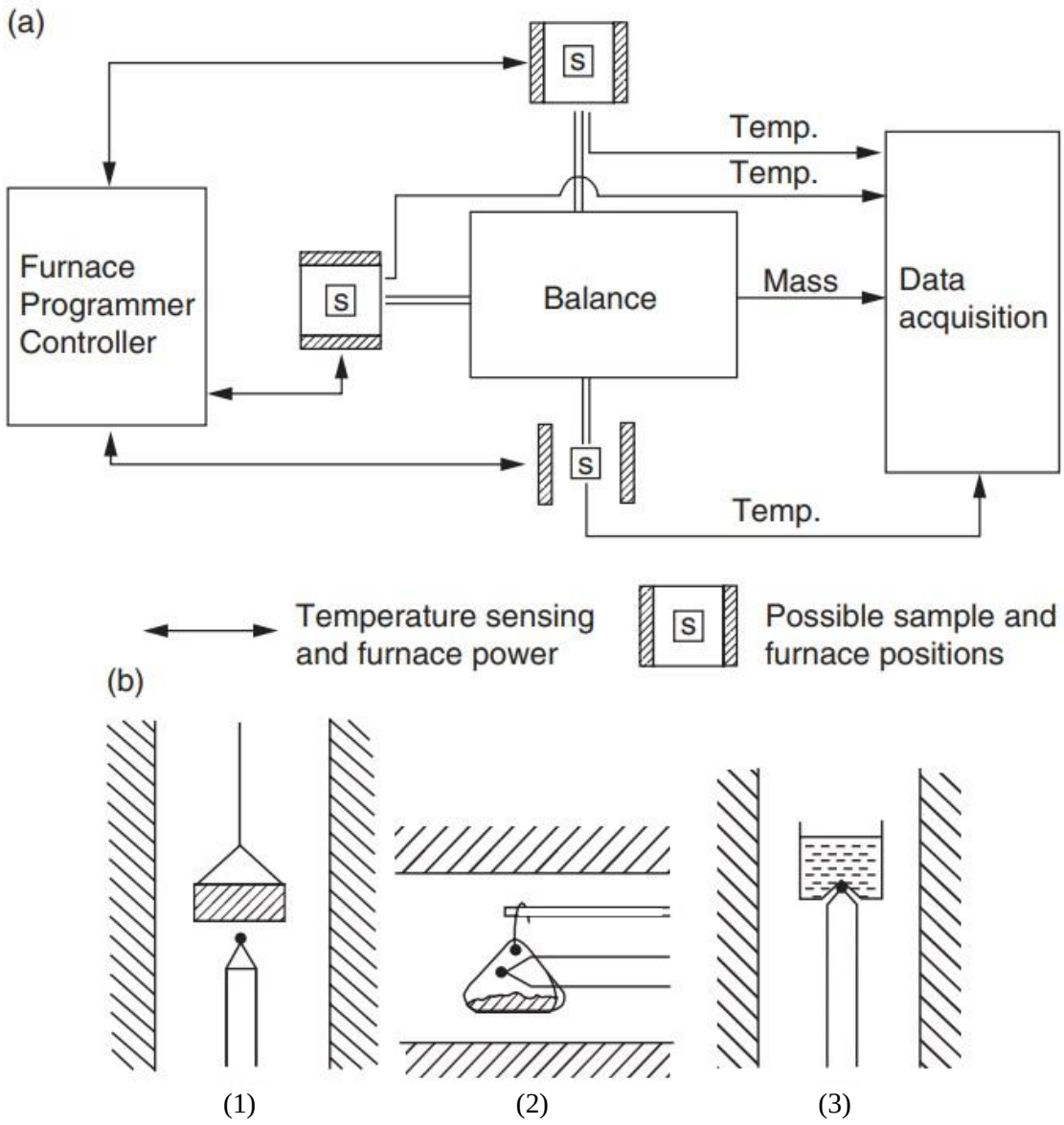

"(a) General arrangement of components in a thermobalance [from Gallagher (1993) with permission of Elsevier]; (b) typical location of thermocouples: configuration (1) top - loading, configuration (2) side - loading, and configuration (3) bottom loading [from Gallagher (1997) with permission of Elsevier." (22)

A typical TGA device can hold several milligrams of substance, heat them for a set temperature, up to 1600 °C or more, at a steady or variable rate, and keep the sample chamber (furnace) under a confined atmosphere of either air or an influx of a given gas (23).

The use of TGA in this work aims to identify the thermal decomposition of levofloxacin as a function of the temperature gradient, until its complete pyrolysis. This serves to later

quantify the kinetic parameters needed for this work, to understand the drug's decomposition and its associated energy values.

However, TGA on its own does not possess the capability to detect or evaluate phase transitions, polymorphic transformations, and/or reactions that possess variable mass changes. Therefore, to get a more comprehensive result, a complementary experiment must be conducted using DSC to account for this incapability, by providing the means to account for the physical changes that TGA does not account for (23).

DSC, as a device and technique, uses heat flow as the analysis method. The device consists of a heating chamber with two sample cells, one of which is for a reference material, and one for the analyte, with a thermometer to evaluate the temperature at each point of the heating process. This information is also relayed to a computer unit to tabulate and graph the results. Figure 4 shows a schematic diagram of the DSC device's cell (22).

Figure 4

Schematic interpretation of DSC device's cell. "Cross section of a Du Pont (now TA Instruments) 910, 2910, and 2920 DSC heat flux cell (Blaine, Du Pont Instruments bulletin; courtesy of TA Instruments)." (22)

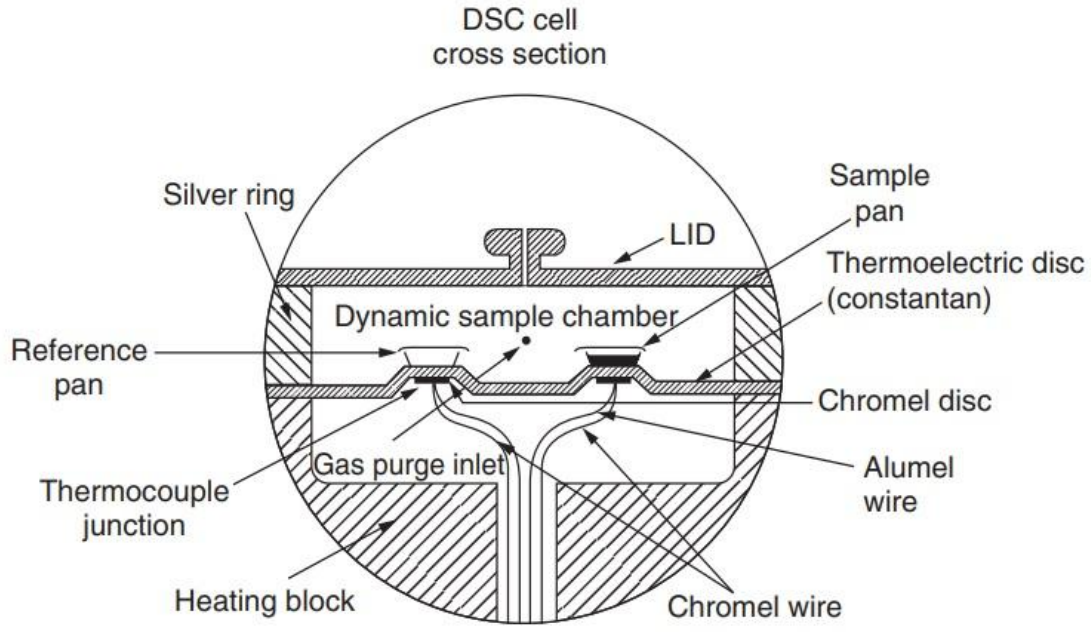

DSC can identify characteristic temperatures, the heat of fusion, the melting and crystallization temperatures, and the heat capacity, more importantly for the interest of this work, DSC can determine the various thermal parameters of chemical reactions (22).

Both devices study the behavior of the material at critical points, like melting, oxidation, and eventually pyrolysis. Which in conjunction with each other and with literature asserts a picture of the thermal behavior of the material. Both devices' heating chambers are equipped with a gas inlet to allow for flushing the chamber with an appropriate gas for the experiment's conditions (22).

From Nisar et al. (20) where they analyzed the thermal behavior, that work emphasized the importance of thermal analysis using TGA and DSC for understanding the reaction mechanism of the drug. That is the reason for this work employing the use of computational calculations as a method to further validate and scrutinize such results and build on previous data from literature.

1.3 Isoconversional methods

The concept of isoconversional kinetics stems from the isoconversional principle, which enables the exclusion of the reaction model from kinetic calculations. This principle posits that, "the process rate at constant extent of conversion is only a function of temperature" (2). This means that any and all reactions where the ratio of reactant depletion is constant, can have their rate be studied through the measurement of the temperature as a function over the reaction period (2). And by going back to the previous point about how the thermochemical and kinetic properties are caused by the electromagnetic interactions within a molecule or intermolecularly, this confirms that the interaction between a material and its surroundings have a direct effect on the intermolecular and intramolecular interactions (2, 4, 17, 21, 9).

Experimentally, the isoconversional analysis requires a determination of the extent of the reactant conversion (α), this is a parameter that determines the rate at which any indicative physical or chemical property of the molecules change between the point of measurement and the reaction termination or equilibrium point, requiring this change to be indicative of reactant depletion or product formation (2).

For purpose of this work, α can be easily calculated by measuring any physical property that varies with the reaction's progression (2). For this work, the reaction progress will be tracked through the change in mass using TGA, which indicated the reactant depletion inside the TGA chamber. α will be determined by dividing the incident mass change (Δm) by the total mass change (Δm_{tot}) that has occurred during the entire process (2).

$$\alpha = \frac{m_0 - m}{m_0 - m_f} = \frac{\Delta m}{\Delta m_{tot}} \text{ ..... [1]}$$

From this it can be assumed that homogenous reactions can be described using the "Reaction -Order model" which suggests:

$$f(\alpha) = (1 - \alpha)^n \text{ ..... [2]}$$

By leveraging the temperature dependence of the isoconversional rate, it becomes possible to estimate the effective activation energy values (E_α) without having to identify or make assumptions about the reaction model (2).

This is to determine the parameters of the main two equations that will tie into the method, and these are [3] and [4] below:

$$\frac{d\alpha}{dt} = k(T)f(\alpha) \text{ ..... [3]}$$

where, t is the time in seconds, T is the temperature in Kelvin, and k(T) is the rate constant. And:

$$k(T) = A \exp\left(\frac{-E_\alpha}{RT}\right) \text{ ..... [4]}$$

of that, A is the preexponential factor, and R is the gas constant.

The Isoconversional method employs a unique rate equation for every degree of conversion and a limited temperature range, ΔT, linked to that specific conversion. By utilizing distinct heating rates, β1 and β2, the approach enables the determination of different rates at the same conversion, according to the following equation:

$$\frac{d\alpha}{dt} = ß \left(\frac{d\alpha}{dT}\right) \text{ ..... [5]}$$

Therefore, if the aim is to calculate the effective activation energy, then plug equation [4] into equation [5] where the temperature dependence would replace the time dependence. This produces the following equation [6]:

$$\frac{d\alpha}{dT} = \left(\frac{A_\alpha}{ß}\right) \exp\left(\frac{-E\alpha}{RT}\right) f(\alpha) \text{ ..... [6]}$$

After obtaining the temperature dependence of the isoconversional rate via a sequence of temperature programs, and applying the previous equations to the data, it can be parameterized by the differential isoconversional equation from Friedman]7] (2):

$$\ln\left(\frac{d\alpha}{dt}\right)_{\alpha,i} = \ln[A_\alpha f(\alpha)] - \frac{E_\alpha}{RT_{\alpha,i}} \ldots\ldots\ldots\ldots\ldots\ldots [7]$$

where (i) is the identity number of the temperature program setting for each of the solutions of the equation.

Another common equation that is used for the determination of E_α is the Kissinger–Akahira–Sunose (KAS) equation (2):

$$\ln\left(\frac{\beta_i}{T_{\alpha,i}^2}\right) = \text{const} - \frac{E_\alpha}{RT_{\alpha,i}} \ldots\ldots\ldots\ldots\ldots\ldots\ldots [8]$$

This will be useful in determining the E_α by plotting the of $\ln(ß\frac{d\alpha}{dt})$ for all heating rates against $1/T_{(K)}$ for the Friedman method, and, $\ln(\frac{ß}{T^2})$ against $1/T_{(K)}$ for the KAS method and finding the slope of the best fit line as will be further explained in Chapter 2 along equation [13].

In reactions where the mechanism is unknown, these methods have proven to be an accurate technique for the determination of the reaction mechanism (24). Within these methods this work takes two counterparts, those are the linear (e.g. KAS) and nonlinear (e.g. Friedman) estimation to the derivative and the integral calculus from Arrhenius equation. And as a byproduct of the result assess the accuracy of both, confirming what other researchers mention about the accuracy of nonlinear methods being greater than that of the linear methods. Since the nonlinear methods use integrals while the linear methods suppose that the kinetics model and activation energy remain the same within the reaction (24).

In their work on metformin, Badran et al. (17) explained the difference between the two methods (KAS and Friedman), they explain that as Friedman equation which is a differential method, and KAS is an integral method. Moreover, they continue to add that Friedman is advantageous over KAS since the first uses no approximation, and may be applied to any temperature program by taking the logarithm of both sides of equation [6]

under different heating rates. This is in alliance with the work of sbirrazzuoli et al. (25) where Friedman was confirmed to give good results, based on their work on DSC.

In the work of Nisar et al. (20) they used Ozawa Flynn Wall (OFW) method of calculating the kinetics and it is a linear approximation of the derivative. And from this, have derived a single activation energy for each of the molecules tested in that work. This study aims to add a theoretical quantum calculation to analyze the results with respect to the experimental analysis. The comparison of the results from both studies should prove the reliability and consistency of the methods used within the scope of this analysis.

A repercussion of this study is the emphasis on the tests of the Friedman method by Badran et al. (17) and Sbirrazzouli et al. (25), by comparison with the KAS results as well as contrasting it with the results of the experimentation by Nisar et al. (20) where the latter used OFW method. Along with the results of computational kinetics, this study should provide more evidence that the Friedman method leads to more accurate and precise results (17).

It has been generally assumed that the activation energy of any gaseous reaction should remain the same over any number of molecules that are present in a sample. However, for a condensed phase, with an unknown reaction mechanism, and while the activation energies of some mechanisms are very close to the activation energy of different, but possible, mechanisms, the determination of a single activation energy for a complex mechanism becomes inaccurate. And this is prevalent in the literature on degradation and pyrolysis of molecules that contain bonds that are close in bond-energies to one another (17, 4, 21, 26, 20).

Therefore, this work hypothesizes there will be multiple activation energy outcomes at different α, which is the result of the work at hand not being a unilateral gaseous medium, that can be expressed in a single step of bonds breaking.

The stages that are indicated by the change in α are: melting, decomposition, overlapping, and oxidation (4). These changes are the points of interest that will be examined for the identification of the physical and chemical changes that occur to the molecule in the conditions of changing the physical environment at hand.

1.4 Wastewater treatment

One of the most widely used methods of wastewater treatment is adsorptive removal, which works by adding an adsorbent to a container of wastewater, and working to thermochemically or electrically attach the waste materials to said adsorbent. However, although adsorption is a beneficial method for treating pollutants, it results in a secondary environmental issue, because, by definition, the process produces solid waste concentrated on the surface of the adsorbent (17).

Nassar et al. (17, 27) solved this secondary waste problem by using what they coined as "nanosorbcats" to adsorb, but then also assist the decomposition or conversion, of pharmaceutical and personal care waste from the wastewater (17, 27).

This work, and the analysis it provides meet the world-wide ambition to create ways to make manufacturing PPCPs move towards better disposal methods. Furthermore, this moves the approach from the cumbersome waste-recycling techniques that don't work for various chemicals, to a more effective upgrading, that may see an engineering take to make it financially viable.

1.5 Waste-to-fuel upgrading

Waste-to-fuel upgrading, or as it sometimes is referred to waste-to-energy (WTE) upgrading, is a process that involves converting various types of waste materials into usable fuel sources (28). This can include both organic and inorganic waste, such as agricultural waste, food waste, plastic waste, and municipal solid waste. The process typically involves several steps, including sorting and processing the waste materials, breaking them down into their component parts, and then using various chemical or biological processes to transform those components into fuel sources such as ethanol, biodiesel, or methane.

Waste-to-fuel upgrading has become an increasingly popular approach in recent years as a way to reduce waste and greenhouse gas emissions, while also generating renewable energy sources (29). Organic waste upgrading can be done through oxidation (air), partial oxidation (steam), photo degradation (photolysis), or thermal decomposition (heat) (17). This work uses thermal decomposition by heating the product under inert gas (Nitrogen), in a TGA machine, to determine the change in composition that takes place as the

molecules gain energy (17). From this the results are to be compared and contrasted with computational analysis of the bond energies at several bonds to determine the molecule's most likely site/s for decomposition. Therefore, determining what useful molecules might be produced.

Waste-to-fuel upgrading technology is significant for addressing waste disposal and transitioning to a sustainable economy, by reducing reliance on fossil fuels, mitigating climate change, and generating employment in renewable energy and waste management sectors (28, 29). Additionally, the method used in this study avoids the unwanted byproducts of conventional adsorption technology by eliminating the need to relocate the solid substances produced during the treatment process (17). This work will not focus on the conversion rates of waste-to-energy from this drug, while instead, it focuses on the thermodynamics that make such a technology possible in the first place.

While most studies on isoconversional kinetics concentrate on polymers and ionic solids or liquids (17), This research will focus on exploring a pharmaceutical compound, levofloxacin (18).This work is in conformation with efforts by Badran et. al. (17) to develop a model technique that may be used to upgrade pharmaceutical waste to fuel, such as ammonia, and/or other products for use as commodities. This work draws significance from the aforementioned contrast to conventional methods, that are only ways to remove chemicals from one part of the environment to another. For this, and even if the economic viability is unclear, this method remains the more permanent solution to the issue of waste disposal or removal.

1.6 Theoretical quantum calculations

Computational chemistry, including the use of programs such as ORCA chemistry software (30–41), can be a powerful tool for studying kinetic chemistry. ORCA is a software package that allows researchers to perform quantum chemical calculations on molecules and materials, which can provide insights into the rates and mechanisms of chemical reactions.

One way to use ORCA for kinetic chemistry is to perform transition state calculations, which involve calculating the energy and geometry of the transition state for a chemical reaction. This information can be used to predict the rate of the reaction, as well as the effects of changes to the reaction conditions or reactant molecules (30).

The computational side of this work focused on the bond-energy analysis of the intramolecular interactions of levofloxacin. This is for the determination of the initial degradation mechanism through the analysis of the lowest bond energy in the molecule, as it would be the easiest to thermally degrade. Along with that, the bond energy of an additional pyrolysis at different sites will be calculated and compared to TGA data. From the latter the researcher determined the site at which pyrolysis of the molecule takes place to cause degradation. The main results expected from the computational analysis are $\Delta H_{activation}$, $\Delta G_{activation}$, and $E\alpha$. These results are determinants of the reaction possibility, energy, and conditions required (4).

The main theory utilized in this work will be the Density Functional Theory (DFT). This is a computational approach used in chemistry to study the electronic structure of molecules and materials through computational analysis (42).

In DFT, the electrons in a molecule or material are treated as a probability density function, rather than as individual particles (3). The theory aims to calculate the total energy of a system based on the electron density, which is derived from the wave functions of the electrons. The electron density is then used to calculate various properties of the system, such as the molecular orbitals, the electron density distribution, and the reactivity of the molecule (42–45). This is all in contrast to the more conventional method of Hartree-Fock, which is based on calculating the wave function of the aforementioned particles, and hence, comes with the limitations to complexity that come with dealing with each particle's wave function.

DFT is a widely used method in computational chemistry, as it provides a practical and efficient way to predict the properties of molecules and materials and visualize these molecules and interactions. It has been used to investigate a wide range of chemical phenomena, including chemical reactions, catalysis, and materials science (42–44).

In their work in 1989, Parr, R.G, and Yang (42) posed the shortcomings of DFT having the need for better approximations of the energy functionals than the ones available at the time. With basis sets having a wider range of accuracies and computational power requirements. This has led a wealth of scientists to venture into forming better basis sets that result in better approximations of the energy functionals.

Therefore, an integral part of the computational process to consider is the basis set that should be used. Basis sets are mathematical functions used to approximate the wave function of a molecule or material, representing the behavior of the electrons in the system. Basis sets are constructed as a linear combination of simpler functions. The choice of basis set has a significant impact on the accuracy and reliability of calculations, with larger basis sets (and more complex ones) providing more accurate results but requiring more computational resources, while smaller basis sets are faster but may provide less accurate results. The selection of a specific basis set often depends on the specific problem being studied and the required level of accuracy (46).

In their work Weigend and Ahlrichs et al. found that it is sufficient to use fewer polarization functions, "especially for DFT treatments" (46). The def2-TZVP is a triple-zeta valance base, that includes only (1p) orbital set for Hydrogen, (1f) orbital set for d elements and partly reduced sets for s elements. Thus, this is sufficient as the researcher of this work was not interested in the excited states of the molecules, so as to conserve computational power without negating the accuracy.

For this work the intended result is to find the most probable bond to break initially, this in scientific terms means the bond that has the lowest energy at the lowest temperature, and that continues to have lowest energy results at higher temperatures, along with a negative Gibbs free energy (ΔG) value indicating its breaking spontaneously at the corresponding temperature. An increase in entropy (ΔS) is expected, as the reaction at hand in all cases produces more molecules and less order.

The resulting files show the calculations run by the program along with their outcomes. The outcomes of interest to this work are:

1. Electronic energy:

This indicates the Single Point Energy (SPE) in Hartrees.

2. Zero point energy:

This indicates the Zero Point Energy (ZPE) in Hartrees.

3. Total thermal correction:

This indicates the thermal correction of enthalpy ($H_{corr.}$).

4. Final entropy term:

This indicates the entropy correction ($S_{corr.}$).

The thermodynamics are calculated based on a set of equations, starting from four aforementioned results of the quantum calculations of the ORCA program (2, 3, 9, 4, 21, 45, 47, 48), and assuming levofloxacin to be the reactant and the fragments at each experiment are the products, these equations become:

$$\Delta H_{0K} = \left(\sum SPE_{prod.} + ZPE_{Prod.}\right) - \left(SPE_{react.} + ZPE_{React.}\right) \quad \text{..... [9]}$$

$$\Delta H_{TK} = \left(\sum SPE_{prod.} + ZPE_{Prod.} + H_{corr.\,TK}\right) - \left(SPE_{react.} + ZPE_{React.} + H_{corr.\,TK}\right)$$
..... [10]

$$\Delta S_{TK} = \left(\sum SPE_{prod.} + ZPE_{Prod.} + S_{corr.\,TK}\right) - \left(SPE_{react.} + ZPE_{React.} + S_{corr.\,TK}\right)$$
..... [11]

$$\Delta G_{TK} = \Delta H_{TK} - \left(\frac{T + \Delta S_{TK}}{1000}\right) \quad \text{..... [12]}$$

where T is the temperature in Kelvin degrees. And each term is used with its corresponding temperature as fit.

From the resulting values an understanding of the molecule's thermochemical behaviour at the given circumstance may be built:

- ΔH_{0K} indicates the reaction change in enthalpy at 0K, and its sign determines the expected heat flow in the system, whether indo-thermic or exo-thermic, which answers this work's question of whether external energy might be needed to sustain the decomposition of levofloxacin.
- ΔH_{TK} indicates the reaction change in enthalpy at a given temperature, for that it determines the heat flow in the system. This is used to analyse the changes that occur to the molecule, if any, when it is not at the extreme circumstance of absolute conditions for practical applications.
- ΔG_{TK} indicates the Gibbs free energy at the given temperature, and magnitude determine the possibility and spontaneity of a bond interaction as of the one being analysed.

- Finally, ΔS determines the change in entropy, which helps determine the reaction's direction of equilibrium, and whether more reactants are likely to stay as initiated or products produced.

Together, these results may be compared and contrasted to the isoconversional results, to determine the validity of the latter. But also indicate whether the reaction at hand is chemically viable or not.

Based on the author's knowledge, and to the best of their knowledge, computational chemical analysis is used for the first time on levofloxacin in this study.

1.7 Fragment selection and molar mass

The selection of possible bonds to break for testing is made through analysis of the larger molecule and similar molecules' behavior. This rules out the possibility of ring-opening, as rings are typically some of the most stable parts of a molecule. This also rules out all of the double bonds within the drug's molecule. This also is supported stereochemical by the outermost bonds being the most exposed to the environment, with inner electrons being shielded by the fields of the outer ones, and the fact that a bond's thermal stability correlates to the space an electron has to move. Therefore, the most likely bonds with the outermost configuration have been selected as seen per [Appendix A].

The selected bonds for dissociation will be assumed to produce two radicals since the severed bond will be considered to be split through homolytic cleavage. Where radicals, or more precisely 'free radicals' are molecules, ions or atoms that possess unpaired valance electrons, or an open electron shell. Homolytic cleavage, is the bond being severed with each of the atoms of the bond taking one of the bonding electrons in the case of single bonds (49). Since this helps detect the strength of each of the bonds through its dissociation energy. And through the work of Ding et al. (49) on homolytic cleavage of $C(SP^2)$-O bonds in ethers and phenols, DFT has been proven to produce good results when it comes to homolytic cleavage.

Within the fragmentations that are produced by the presumed bond dissociations, each of them has been given the name of the atom it possesses out of the bond's atoms, based on the labels given to the levofloxacin molecule by the Avogadro software. The molar mass of each of the produced radicals, are analyzed per one. These molar masses will then be

calculated as a percentage of the full levofloxacin molecule's molar mass. After which the percentages will be compared to the percentage of mass lost during the TGA analysis to prove whether or not a certain fragment left the molecule. And to conclude which of these dissociations are the ones to actually occur during the heating process.

In their report, Prohaska et al. provided the standard 'atomic weights' of the elements (50), which is for this application, equal in value, but not identical, to the molar mass of each element in grams per mole (g/mol). As this is, to the best of the researcher's knowledge, the most recent standardization at the International Union of Pure and Applied Chemistry (IUPAC), their work has been used to determine the molar mass of the molecules and fragments examined in this work.

The molar mass of each of the elements present in levofloxacin is shown in Table:

Table1

Standard atomic weight of elements

Element	Symbol	Abridged standard atomic weight (Dalton)	Uncertainty value ±
Hydrogen	H	1.0080	0.0002
Carbon	C	12.011	0.002
Nitrogen	N	14.007	0.001
Oxygen	O	15.999	0.001
Fluorine	F	18.998	0.001

The molar masses are then calculated based on the atomic weights as seen per Table in the following chapter, as the summation of the atomic weight multiplied by the number of atoms per molecule or radical.

1.8 General commentary on theoretical background

According to previous studies, levofloxacin was analyzed in accordance to its chemical properties through the work of researchers such as Pereira et al. (13) who found the drug to be susceptible to polymorphism. Others studied the physical properties, such as Nisar et al. (20) who looked into the effect of thermochemical changes on the drug's properties, through one of the isoconversional methods. This work, looks into the chemical and

physical changes that occur during the decomposition of levofloxacin through different estimations using isoconversional kinetics and computational calculation models. This work builds on the efforts by Badran et al. (4, 17, 21, 9) to find a mechanism to treat pharmaceutical waste.

The devices used for the experimental analysis are TGA and DSC, both of which are indicators of the critical points of interest at which changes occur to the chemical or physical properties of the drug. These critical points will be a result of the graphing of the data produced by each device and the curves that result from this graphing.

In correlation with the work of previous researchers (4, 17, 21, 9) the results calculated from the devices in the experimental analysis will provide the activation energy, as a result of the chosen equations (KAS and Friedman).

Since the drug has been stated in O'Neil's work in the Merck index (51) to be combustible when mentioning its melting point, this hints that the molecule may oxidize in a manner that causes gaseous compounds to be released. This may in turn cause the experimentation results of the TGA under ambient air to have undesired outcomes, and the assessment of the results of this part will rely on this information so as to sustain an accurate depiction, without allowing for relative systematic error, and or phantom points of data that combustion within the small chamber of a TGA device may cause.

The computational analysis of this molecule would possibly provide the most likely mechanism of action of this drug's molecules. This is through the assembly and application of the well-known calculations of quantum analysis, i.e. finding the density functions of electrons within each atom, and by extension finding the overall potential energy within the molecule.

The selection of the method and basis set will be determined based on the aforementioned criteria, which is having the most accurate results possible while not causing the computational power to be out of hand for the time and devices of this experiment.

The dissociation of several bonds will be examined in the computational analysis. These dissociations will create fragments consisting of two radicals each, one at each side of the bond. These fragments will be named after the atoms at each end of the bond based on the labels given to said atoms from the Avogadro software as shown in Appendix A.

The computational results will be compared and contrasted with the results from the experimental work to provide a measure of accuracy and reliability. While also giving the final verdict on the most probable bond dissociation to occur through the thermal processing of the drug. This is in accordance with analysis used by Badran et al. (4, 17, 21, 9) on other chemicals from the pharmaceutical and personal care sector.

These conclusions may allow for work in the environmental sector to build on them for better and more effective methods of wastewater treatment and/or waste-to-fuel upgrading. Although this may be difficult to assess, from a feasibility view for the commercial and engineering sectors without further quantification and more data on other contaminants' behavior, this work aims to be a step towards achieving a model that can be used for other chemicals in the industry to better understand them and their possibility for the application of the "nanosorbcats" technology mentioned by researchers in the field (17) to solve the issue of adsorptive removal of waste producing secondary waste that has to be re-processed.

Chapter Two

Methods

In this work, the decomposition of levofloxacin was examined as a function of its thermal and kinetic behavior using the isoconversional methods and theoretical analysis of the molecule's bond energies. As a way to determine the changes that take part when it is subjected to heat, and the products of its pyrolysis and possibility that fuel may be produced from this reaction.

2.1 Experimental thermochemical analysis, using isoconversional methods

For this research experiment, the temperature dependence of the isoconversional rate was obtained experimentally by performing a TGA series of runs at different temperature programs.

The TGA device used for this work was a SANAF TGA (52). Available at the physical chemistry laboratory at An-Najah University (Nablus-PS).

In each procedure, approximately 20-22mg of levofloxacin hemihydrate powder, obtained from Sigma Aldrich (CAS: 138199-71-0), were subjected to varying heating rates ranging from 15 - 30 °C/min under a continuous N_2 gas-flow-rate of between 65-85 mL/min, while heating the sample from ambient temperature to 800 °C, holding at 110 °C for 10 minutes each time to account for water impurities evaporation from the sample. The device was set to produce a mass reading every second for the period of the heating, correlated to a temperature reading at every point.

Another set of procedures was conducted with the same approximate mass and subjected to heating rates ranging from 10 to 20 °C/min under air, holding at 110 °C for 10 minutes to allow for water impurities' evaporation from the sample. The device was set to produce a mass reading every second for the period of the heating, correlated to a temperature reading at every point.

The TGA device was calibrated beforehand by adjusting for the weight of the appropriate disposable crucible. At which point the indicated mass of any single run was the mass of levofloxacin sample. The device was then flushed with N_2 gas to remove any residual

particulate matter or residual air from previous use, and the drug put in the crucible on the TGA machine's balance compartment.

The analysis of the outcome data was conducted using Microsoft Excel and Origin 2023 software programs (53).

The results of the TGA analysis were then tabulated. Regions of interest to this work were taken from the overall data to make for better comprehension and graphing of the figures.

To confirm the TGA results a sample from the same drug was sent to the University of Jordan for DSC analysis, the result confirmed the hypothesis at hand and confirmed the accuracy of these results. The device used was a NETZSCH DSC 204 F1.

The TGA experiments were conducted at a flow rate of 65-85mL/min, while the DSC experiment was conducted under a flow-rate of 20-60mL/min.

These runs produced a correlation plot of mass and temperature, which were then converted into the α and temperature plot by measuring α as ($\Delta m/\Delta m_{tot}$) [eq (1)], this means it is an indication of what the conversion rate of mass was between any point and the total change that occurs over the whole run.

The results of all heating rates were then graphed using Origin software and ranges of constant α between the different heating rates were then removed to focus on the points of well separated α for each of the heating rates.

In their work, Badran et al. (4, 9, 17, 21, 47). considered certain parts of the α graph to be the region of interest to the experimentation, these regions were selected based on their α changing in a consistent manner, this consistency provides a more accurate estimation when solving for the isoconversional equations. Moreover, these regions allow for the curvature of the α graph to show more obvious critical points of change within the graphs, for identification of the points at which the properties change. This is due to the production of an overlap in the regression of R^2 within a certain range of α, which hinders the application of the isoconversional method if the steps are not well-separated (4, 9, 17, 21, 47).

These regions were temperature ranges as follows:

1. For experiments done under N_2 medium the temperature range was selected to be 120-550 °C.
2. For experiments done under air medium the temperature range was selected to be 115-500 °C.

The resulting data was a new range of mass, which prompted the adjustment of α based on the new initial and final masses. Therefore, the new α was measured for each point.

From there, dα/dt was calculated using Microsoft Excel's internal calculator, for each step, as it means the difference in α divided by the difference in time for each given step.

From there the data was summarized, for better comprehension, as the thousands of readings from the TGA device had some repetition over the smaller intervals. Therefore, a smaller table of the calculations was made, where the taken α points were in intervals of 0.05 starting from α = 0.10 up to α = 1.00.

The logarithm $\ln(ß\frac{d\alpha}{dt})$ was measured for each step also using the internal algorithm within Microsoft Excel. Followed by 1/T in Kelvin (converted assuming $T_{(K)}=273+T_{(°C)}$).

The terms A_α and f(α) remain unchanged for any given α for the isoconversional methods.

Therefore, for the Friedman method, the activation energy may be calculated from the slope of the best fit line of the plot of $\ln(ß\frac{d\alpha}{dt})$ for all heating rates against $1/T_{(K)}$ for all heating rates at any given α.

The resulting equation is:

$$E_\alpha = \frac{(-slope \times R)}{1000} \quad \text{.....[13]}$$

And the square coefficient of determination (R^2) of the plot of $\ln(ß\frac{d\alpha}{dt})$ against 1/T(K) product is then calculated using the internal algorithm within Microsoft Excel for each of the heating rates.

As for the KAS method, $\ln(\frac{ß}{T^2})$ was calculated through Microsoft Excel and plotted against 1/T(K), the slopes of the best fit lines were then found with the same program, and then E_α was calculated using [eq 13] with the same program.

In the KAS method R^2 was calculated for the plot of $\ln(\frac{ß}{T^2})$ against 1/T(K) with the same algorithm as before within Microsoft Excel.

The effectiveness of this method has been demonstrated in generating crucial information that were utilized in analyzing the kinetics and mechanism of a reaction, particularly through the isoconversional methods of KAS and Friedman methods (17). The error margins for which were calculated using the relative standard deviation (RSD), which is a ratio of the dispersion off of the mean, through the algorithm within Microsoft Excel software.

2.2 Theoretical quantum calculations

For this application, the bond dissociation energies (BDE) of several bonds were determined by comparing the potential energy of the anhydrous levofloxacin molecule to the potential energy of the fragments produced by the bond dissociation. From there this led to the determination of the bond dissociation energy for some of the given bonds, and concluded the most-easily broken bond of the molecule.

The anhydrous form was studied in place of the hydrated versions due to its relative simplicity which would reduce the computational power needed for this work, along with being enough to answer to the main goal of this experiment.

The levofloxacin molecule was split into fragments along its outermost single bonds, since these bonds would be the easiest to break while also causing the molecule to lose mass for the purposes of this work. The fragments were given the labels as shown by figure 5 (2D) and Appendix A (3D).

Figure 5

Expected bond dissociations of levofloxacin for analysis in the quantum calculations' section of this work

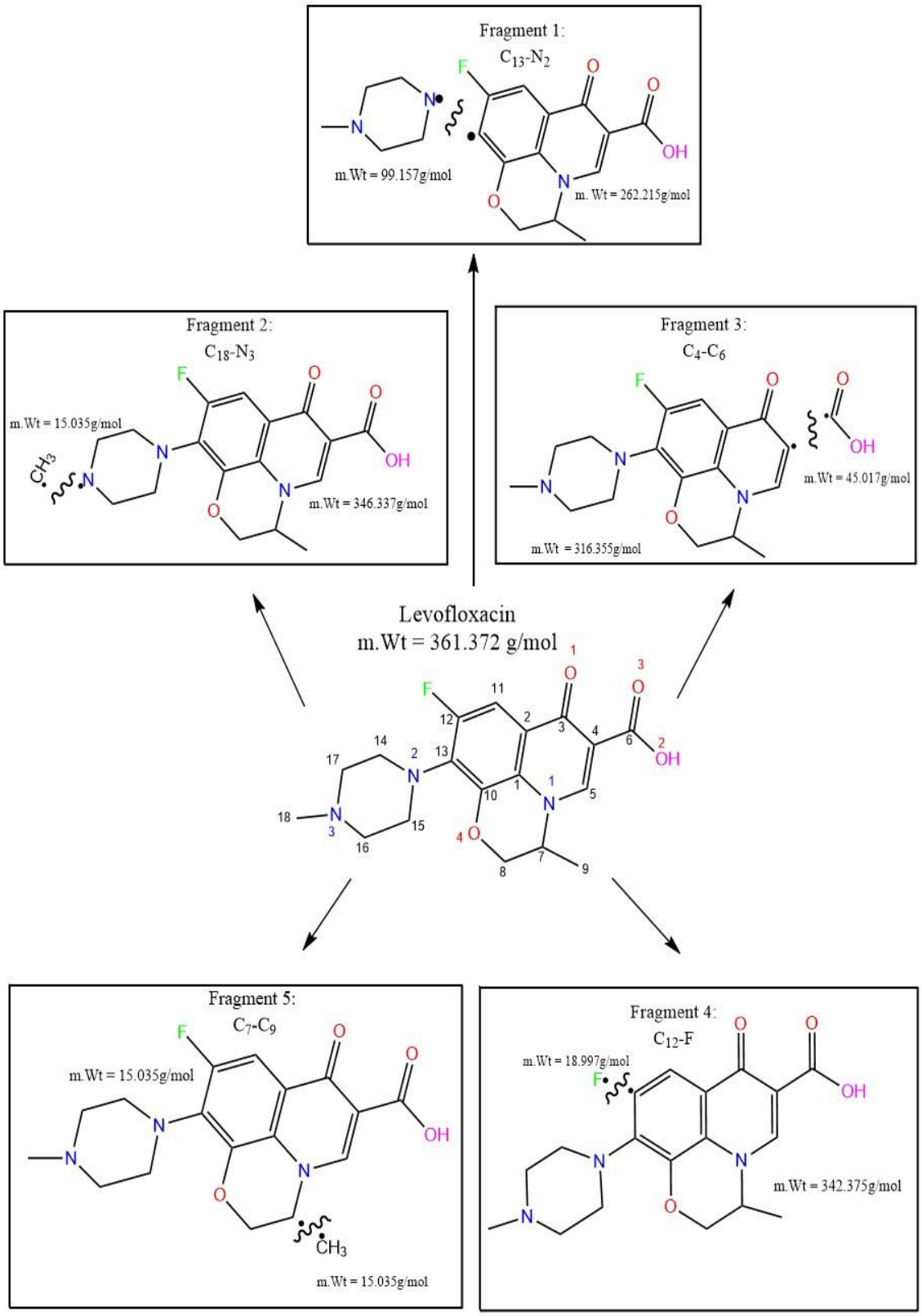

ORCA 5.0.4 program was used to determine the kinetics of the molecules. Which consist of BDE, and thermochemical data (30). The basis set used was def2-TZVP.

The quantum computation for each of the fragments was held at different temperatures of (0K,400K, and 700K) to determine the spontaneity of decomposition under different thermal conditions.

The input files were programmed by drawing the molecule in Avogadro software (54) and retaining the input file from the relevant menu under 'ORCA input' option, the results were as shown per the example Figure 6.

Figure 6

Example: content of input file for ORCA program, with matrix of the atom positions for levofloxacin molecule. (Adjusted for page length constraint, due to atomic position matrix being produced as a list lengthwise)

```
# Levox_Temp298&400&700_opt_freq_01
! Opt Freq RKS M06 def2-TZVP AutoAux
%freq Temp 298, 400,700
end
%PAL NPROCS 24 END

* xyz 0 1
 C 0.65943 0.21659 -0.22196                H 1.71194 -3.02310 -0.00647
 C 0.57320 -1.18314 -0.09307               C 3.11616 0.06797 -0.37313
 C -0.69151 -1.78307 0.05996               F 4.08906 -2.14306 -0.20669
 C -1.85215 -0.98126 0.09461               N 4.40747 0.69597 -0.51768
 C -1.70752 0.41021 -0.02406               C 5.50313 0.07848 -1.25379
 N -0.47987 0.98686 -0.18503               C 4.72648 1.97849 0.09691
 O -0.77941 -2.99611 0.16876               H 3.90062 2.37658 0.71894
 C -3.21743 -1.56029 0.26171               H 4.97380 2.71698 -0.69678
 O -4.29803 -0.74951 0.29232               C 5.93993 1.78973 1.01695
 H -5.19303 -1.10195 0.39912               H 5.22364 -0.88253 -1.72630
 O -3.37644 -2.76740 0.37160               C 6.69950 -0.09506 -0.31655
 H -2.58737 1.04242 0.01372                H 5.79832 0.75454 -2.08628
 C -0.38826 2.46038 -0.26173               H 6.43723 -0.81851 0.48907
 C 0.86634 2.85702 -1.04871                N 7.07111 1.21455 0.25912
 C -0.37104 3.04905 1.15324                H 7.54842 -0.51125 -0.90250
 H -1.26308 2.88142 -0.80744               H 5.65751 1.11598 1.85889
 H 0.49854 2.66472 1.72789                 H 6.22137 2.77958 1.43933
 H -1.30288 2.77285 1.69060                C 8.24937 1.07401 1.12645
 H -0.31074 4.15726 1.10630                H 9.10873 0.67938 0.54269
 O 1.96277 2.17865 -0.55918                H 8.04442 0.38716 1.97783
 H 1.04111 3.95376 -1.03828                H 8.55043 2.06609 1.52636
 H 0.71879 2.54527 -2.10682
 C 1.92362 0.83602 -0.37273
 C 1.75050 -1.94542 -0.11177               *
 C 2.99918 -1.33712 -0.24651
```

From the computation results the most probable products of the decomposition/ pyrolysis were predicted, and therefore, the temperature of the production of each of them. Those were paralleled with the experimental isoconversional data to determine the most-probable reaction mechanism.

The results of the computational data mentioned previously in chapter one, were the energy and entropy values, these were calculated according to equations [9-12] and tabulated to find the difference and compare them. While this provides the lowest energy bond, which means the easiest one to break. Moreover, the energy of the bond is compared to the energy from the KAS and Friedman methods mentioned previously to decide which one correlates to the computational results, and therefore is the more accurate estimation to the actual energy value.

2.3 Mass loss analysis

The molecular formula was analyzed to obtain the molecular weight, as listed per Appendix A, the considered molar mass of each molecule and fragment is the sum of the standard atomic weight of each of the elements multiplied by the number of atoms of said element in the molecular formula of said molecule or radical. An electron's mass is infinitesimally small. Or as Atkins and Paula put it in their book on physical chemistry, on page 755, "virtually 0" (3). So, it is usually disregarded in molecular mass calculations. For this work the mass of electrons in the case of radicals was disregarded relative to a molecule with filled electronic shells, and the atom within a radical is considered indiscriminately of it having one less electron than it would with a filled shell.

These molar masses are useful for the identification of the fragments that are omitted during the mass loss steps of the experimental analysis (TGA). With knowledge of the percentage that each of these fragments represent of the whole molecule, match that with the percentage lost during the heating within the TGA, and deduct if it matches any step within the molecule, therefore if it is possible for that fragment to have been dissociated from the larger molecule, meaning the bond it belongs to has been dissociated.

The molar mass of the molecules at hand follows aforementioned calculation of summing up the multiplication of the atomic weight by the amount of said atom within a given molecule. As seen in Table 2 according to the molecules shown in figure 5 and Appendix A.

Table 2

Molar mass of levofloxacin and its dissociated fragments. Where the radicals produced in each fragment were named after the atom that remained within them as a result of the dissociation based on the labels given by Avogadro software to the atoms

Molecule		Number of atoms					Calculated molar mass
		H	C	N	O	F	
		1.0080	12.011	14.007	15.999	18.997	
Levofloxacin		20	18	3	4	1	361.372
Fragment 1	C13	9	13	1	4	1	262.215
	N2	11	5	2	0	0	99.157
Fragment 2	C18	3	1	0	0	0	15.035
	N3	17	17	3	4	1	346.337
Fragment 3	C4	19	17	3	2	1	316.355
	C6	1	1	0	2	0	45.017
Fragment 4	C12	20	18	3	4	0	342.375
	F	0	0	0	0	1	18.997
Fragment 5	C7	17	17	3	4	1	346.337
	C9	3	1	0	0	0	15.035

Chapter Three

Results

3.1 Experimental thermochemical analysis, using isoconversional methods

The experimental part of this study produced thermochemical and kinetic data, of which each parameter was graphed and tabulated according to their relevance to each other and their respective role in the calculation of the isoconversional methods applied from equations [1-8, 13].

Figure 7

TGA mass loss and DTG results of Levofloxacin at different heating rates under N_2 gas, Corrected for temperature range between 120-550 °C

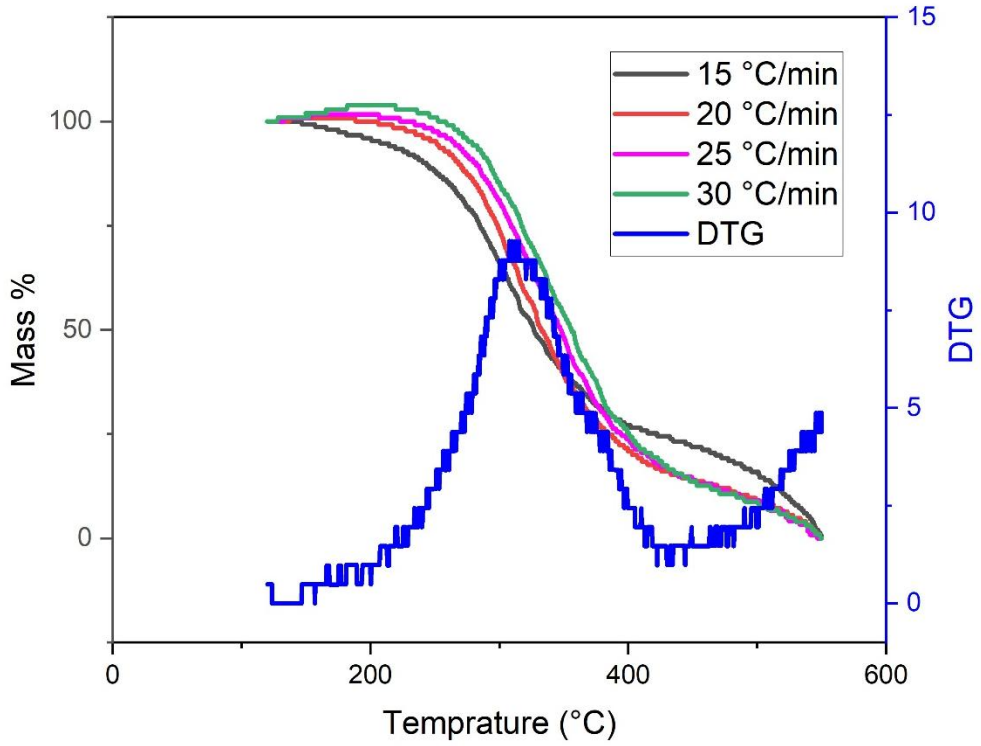

Figure 7 shows two distinct mass losses. The first is at the interval between 235-312 °C, which can be analyzed through isoconversional methods. However, the second at ~350 °C shows overlapping. Therefore, the second mass loss cannot be studied using isoconversional methods (17).

The raw outcomes of the experimental part were as shown in the data pulled from the TGA device. The device constructs a table of Time, temperature, and mass percentage for

each interval given, which was one reading per second. And from the mass percentage a plot of α was calculated based on eq. [1].

From there, dα/dt was calculated as the change in α at each step divided by the change in time for the corresponding step. Which in this case was equal to the change in α, since the time interval was one second between each reading for the device.

The results of the TGA were thousands of readings, for each experiment at the different heating rates, corresponding to each second of the program while it was run during each experiment. The data was then summarized, in intervals of α = 0.05 starting from α = 0.10 up to α = 1.00, for better comprehension, producing a table of α, temperature, dm/dt, and dα/dt. The tabulation and calculation formulas were done using Microsoft Excel's built in calculation tools.

The resulting Table 3 represents the Microsoft Excel page.

Table 3

Summarized TGA data between α = 0.10-1.00 in intervals of 0.05, with dm/dt and dα/dt, created through Microsoft Excel, for experimentation runs under N_2 ga

	15°C/min			20°C/min			25°C/min			30°C/min		
α	**T(°C) (15)**	**dm/dt**	**dα/dt (15)**	**T(°C) (20)**	**dm/dt**	**dα/dt (20)**	**T(°C) (25)**	**dm/dt**	**dα/dt (25)**	**T(°C) (30)**	**dm/dt**	**dα/dt (30)**
0.10	240.6	-0.4900	0.007	266	-0.510	0.008	279.8	-0.47	0.008	291	-0.5500	0.010
0.15	259.4	-0.4900	0.007	281.4	-0.510	0.008	290.7	-0.47	0.008	298.5	-0.5500	0.010
0.20	273.3	-0.4800	0.007	289.8	-0.520	0.008	300.7	-0.46	0.008	310.1	-0.5500	0.010
0.25	283.9	-0.4900	0.007	297.8	-0.510	0.008	308.4	-0.47	0.008	317.1	-0.5500	0.010
0.30	293	-0.4900	0.007	303.9	-0.510	0.008	315.8	-0.47	0.008	324.9	-0.5500	0.010
0.35	301.7	-0.4800	0.007	312.6	-0.510	0.008	324.8	-0.46	0.008	332.8	-0.5500	0.010
0.40	308.7	-0.4900	0.007	318	-0.520	0.008	332.1	-0.47	0.008	338.9	-0.5500	0.010
0.45	316.1	-0.4900	0.007	326.5	-0.510	0.008	339.7	-0.47	0.008	347.1	-0.5500	0.010
0.50	326.3	-0.4900	0.007	331.5	-0.510	0.008	347.4	-0.46	0.008	355	-0.5500	0.010
0.55	336.3	-0.4900	0.007	340.6	-0.510	0.008	353.4	-0.47	0.008	361.5	-0.5500	0.010
0.60	348	-0.4800	0.007	348.2	-0.520	0.008	360.9	-0.23	0.004	370.5	-0.5500	0.010
0.65	364.4	-0.4900	0.007	357.5	-0.510	0.008	369.6	-0.47	0.008	378.2	-0.5500	0.010
0.70	381.1	-0.4900	0.007	367.8	-0.510	0.008	378.9	-0.47	0.008	385	-0.5500	0.010
0.75	415.1	-0.4900	0.007	384.9	-0.510	0.008	391.3	-0.46	0.008	399.2	-0.5500	0.010
0.80	467.6	-0.4900	0.007	402.9	-0.520	0.008	410.1	-0.47	0.008	413.2	-0.5500	0.010
0.85	501.1	-0.4900	0.007	433.1	-0.510	0.008	439.2	-0.47	0.008	442.8	-0.5500	0.010
0.90	522.3	-0.4900	0.007	483.4	-0.510	0.008	486.6	-0.47	0.008	484.1	-0.5500	0.010
0.95	539.1	-0.4900	0.007	528.4	-0.510	0.008	522.3	-0.46	0.008	524.1	-0.5500	0.010
1.00	550.1	-0.4900	0.007	548.7	-0.520	0.008	546.8	-0.47	0.008	549.1	-0.5500	0.010

From these results the table was reduced to another ranging from α = 0.10 to α=0.55 with intervals of 0.1 and these were the points considered for the Arrhenius plots. This

selection was based on the overlap in the regression of R^2 as mentioned previously, since the selected steps were the ones with observable separation within the range of α.

The region of interest was considered 120-550 °C for experiments under N_2, and 115-500 °C for experiments under air. These results were graphed in Figure8 and Figure9, the difference between the two results is one was for results of experiments conducted under N_2 gas corrected for α correlated to temperatures ranging between 120-550 °C Figure8, and the other was for experiments conducted under ambient air corrected for α correlated to temperatures between 115-500 °C Figure9. These plots were graphed using Origin software.

Figure 8

Change in α as a function of the change in temperature during TGA under N_2 gas, α graphing corrected for each ß to unify temperature range between 120-550 °C

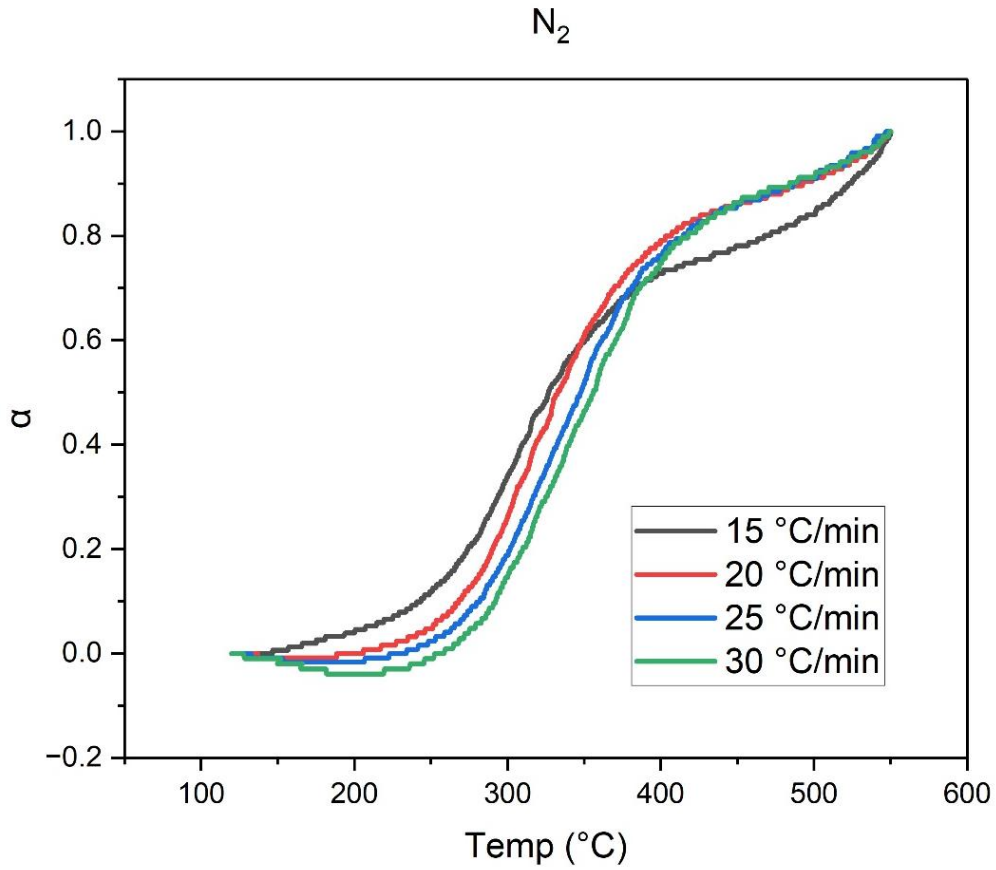

Figure 9

Change in α as a function of the change in temperature during TGA under Air. α graphing corrected for each ß to unify temperature range between 115-500 °C

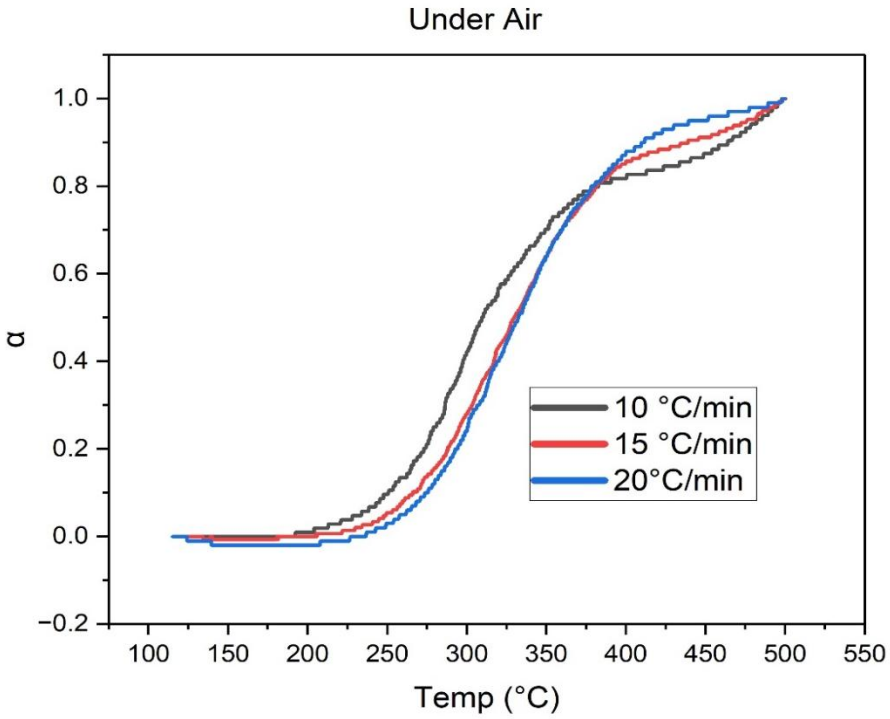

The region of each graph was selected based on how indicative it is of correlation between the different temperature programs from Figure8.

The results' reliability was confirmed by the correlation of each of the lines to the change in temperature set by the program at each run of the experiment (temperature program), and for these purposes the experiment's original data is shown to be more reliable for the runs conducted under N_2 condition than the ones under air. This hints at the possibility of changes that may have occurred due to the denaturing of the compound by the element of oxygen being present in air. And, by extension, that the thermo-oxidative decomposition of the molecule may have resulted in a more profoundly complex manner of action or reaction mechanism.

For this reason, the data under N_2 condition were selected as the primary set of data for further calculations to be conducted, having proven that thermo-oxidative reactions are possible, but also have a separate and equitable set of mechanisms that take place.

The graph in Figure8 shows a change in curvature, indicating a critical change at around 120 °C, which is indicative of the area after water evaporation, then at around 225 °C-

230 °C, which is indicative of the melting and decomposition of the molecule (51), and complete decomposition after around 350 °C.

In their work on the crystallography of levofloxacin Pereira et al. (13) and Wei et al. (14) discussed the polymorphism of the levofloxacin molecule and how it affects the kinetics and degradation.

The crystal in the original sample was susceptible to humidity from the air exposure as indicated from the dehydration mass loss of more than 5% of the total mass. While the levofloxacin hemihydrate should not contain more than 5% water by mass, as the molar mass of levofloxacin is 361.372 g/mol and water is 18.015g/mol. In this case, however, that is not an issue for the objective of this work, as the dehydration takes place before any other changes studied for the aim.

For each experiment under N_2 gas the aforementioned calculations [eq 1-7], along with the evaluation of their respective RSD, were conducted using Microsoft Excel software to reach the data from Table4.

Table 4

Isoconversional results for levofloxacin using TGA under N_2 using the Friedman and KAS methods

	Friedman				KAS			
α	slope	Eα (kJ/mol)	R2	RSD (Eα)	slope	Eα (kJ/mol)	R2	RSD (Eα)
0.10	-5942.17	48.33	0.98	7.95	-2866.28	23.31	0.97	4.52
0.15	-7956.26	64.72	0.97	10.51	-4168.89	33.91	0.95	6.67
0.20	-9139.46	74.34	0.99	6.08	-4877.87	39.68	1.00	1.97
0.25	-10328.16	84.01	0.99	4.67	-5709.88	46.44	1.00	0.72
0.30	-10905.00	88.70	0.99	6.84	-6089.64	49.53	0.99	2.51
0.35	-11517.71	93.69	0.98	9.01	-6415.79	52.19	0.99	2.48
0.40	-11490.94	93.47	0.95	12.09	-6549.57	53.27	0.98	4.81
0.45	-11810.12	96.06	0.97	9.20	-6677.27	54.31	0.99	3.47
0.50	-12008.07	97.67	0.91	17.05	-6909.72	56.20	0.92	9.01
0.55	-14447.56	117.52	0.92	15.94	-8418.06	68.47	0.92	9.16

The Friedman results at $\alpha = 0.55$ was 117.52 kJ/mol, that is similar to the results approximated by the work of Nisar et al. (20) where they estimated the activation energy to be 118.05 kJ/mol with the OFW method.

The 'slope' values are the slopes of the plot of the best fit mentioned in Chapter 2, equation [13].

The (R^2) values of the Friedman method are ranging between 0.91-0.99 for the given α range between 0.10-0.55, while the KAS method shows R^2 values ranging between 0.92-1.00 for the same range of α.

The E_α values were obtained through [eq 13]. The values of which were between 48.3 – 117.5 kJ/mol for the Friedman method. And between 23.3 – 68.5 kJ/mol for the KAS method.

The RSD values of E_α showed a significant difference between the two methods, with the Friedman method having E_α RSD values between 4.67 and 17.05, and the KAS method having E_α RSD values between 0.72 and 9.16.

The Arrhenius plots of the data were obtained using the Friedman and KAS methods as shown per Figure10, and Figure B.1 in Appendix B a good linear fit was obtained for all points, and are well separated for α between 0.10-0.55.

Figure 10

Arrhenius plot of the Friedman method results, with linear fitting. The R^2 value are tabulated in Table4

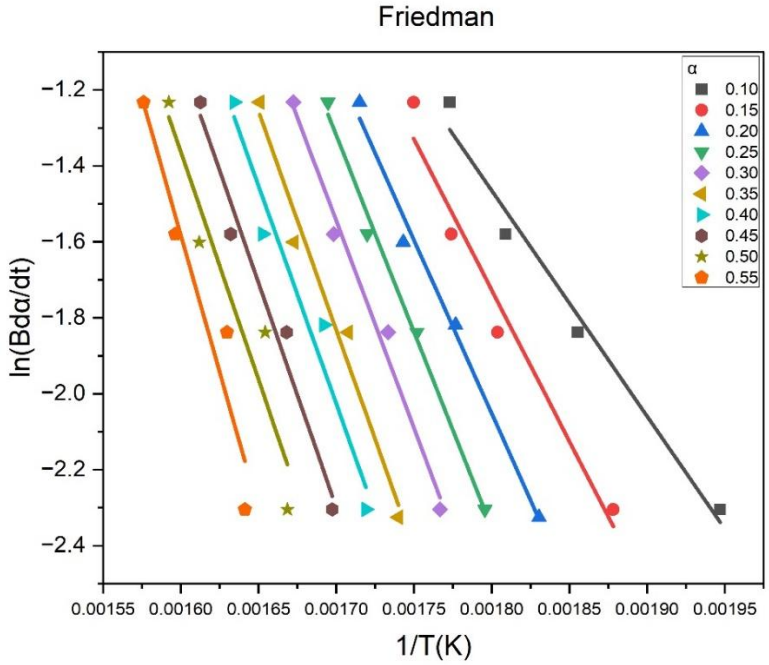

The effective activation energies were obtained from the slopes of the linear fitting according to eq [7] and eq [8], using eq [13] and plotted through Origin software.

A comparison was conducted between the two calculation methods together, along with their respective error margins based on the RSD of E_α in Figure B.2 in Appendix B, this shows a different E_α for each α, that is because these points each depict a single moment within a complex reaction mechanism and the polymorphism of the molecule throughout the reaction mechanism means that there may be several forms of the crystal at each point, with each having a distinct E_α and interaction model (9, 26):

The dependence of the E_α on α is shown in Figure B.2 In Appendix B the deviations in E_α values estimated using the Friedman and KAS methods can be explained by the fact that differential isoconversional methods such as Friedman method used in this study are sensitive to experimental noise, this in turn limits the use of the Friedman method in condensed phase reactions, as mentioned by Badran et al. (17) within the scope of their work on metformin.

Additionally, as mentioned in chapter one the E_α values obtained by the Friedman method are independent of the heating rate. This gives this method an advantage as it reduces the effects of systematic error in evaluating the activation energy values. This has also been evident in the work of Badran et al. on metformin (17), where they reference further proof from the work of Sbirrazzuoli et al. (25) in the simulation of kinetic methods in DSC, where the latter prove the good performance of the Friedman method.

As evident in Figure B.12, the E_α is changing, showing an increase with respect to the change in α. This hints at the fact that different steps of the experiment have different effective activation energies. This in turn is a result of each step probably consisting of a different composition, be it because of stereo chemistry, physical state, or different chemical compounds breaking down or forming within the reaction apparatus throughout the decomposition steps. This is consistent with the work of Badran et al. (17) on metformin, and shows promise in the consistency of the model to be produced from this kind of experimentation. This point will also be discussed further in light of the computational data in chapter four.

3.2 DSC analysis

The DSC examination was carried out on a sample of 5.422 mg of the levofloxacin hemihydrate. And the 'atmosphere' remark denotes the gaseous medium under which the experiment was conducted, which is N_2 gas at a flow rate between 20.0ml/min and 60.0 ml/min.

The temperature range is shown to be between ambient temperature and 400 °C, and the DSC scale is shown in units of milliwatts per milligram (mW/mg).

The scale was upright, meaning the exothermic peaks are towards the positive side of the Y axis (DSC scale) and the endothermic peaks are towards the negative side of the Y axis.

As Figure B.3 in Appendix B shows, there are three distinct peaks. Each of which indicates a certain direction of the heat flow in relation to the reference material.

The DSC was conducted under N_2 gas, which cannot react with levofloxacin. This rules out the possibility of external oxygen reacting with the drug.

The first peak at 106.8 °C is an endothermic peak that indicates the dehydration of the sample of the drug. This shows that the molecule lost its water content. Which is expected when temperatures reach around 100 °C.

The second peak at 238.4 °C is also an endothermic peak that corresponds to the dissociation of molecular attractions. The second peak is also shouldering, which means that it consists of multiple overlapping peaks. This is to be expected as mentioned in the Merck index (51) which sets the melting point of levofloxacin at 225-227 °C. Where right after the melting it is evident there is decomposition indicated by the large peak.

The molecule appears, in both cases of endothermic peaks, to have consumed energy to break molecular attractions; intermolecular attractions in the case of dehydration and melting and intramolecular bonds in the case of decomposition, resulting in these endothermic peaks.

The third peak at 348.6 °C is an exothermic peak that indicates the formation of new bonds. This resulted in the release of heat as evident by the detection of the aforementioned exothermic peak.

Compared to the result of similar analysis by Nisar et al. (20), the peaks in Figure B.3 appear slightly different in the temperature ranges. However, the flow of heat within the system seems to correspond with the same phenomena; dehydration, melting, and decomposition, where the results were endothermic peaks in both experiments. On the other hand, Nisar et al. (20) attributed their exothermic complex peak to the formation of the drug's polymorphs out of the anhydrous form (4, 17).

3.3 Theoretical quantum calculations

The quantum calculations were performed on the anhydrous form of a single molecule of the drug. The resulting quantum calculations were in the form of software, of which the outcome was taken.

The work of Badran et al. on other compounds revealed that it is possible to analyze the bond energy by comparing the potential energy of a molecule with the potential energy of the molecules resulting from breaking any of its bonds (4, 17, 21, 9, 47).

By using the ORCA program, the results were detailed evaluations of the molecule's atomic positions. Converging on the most probable and chemically viable stereochemistry. The configuration of the atomic structure, and therefore the bonding within the molecule could be calculated. Which the program also evaluates and produces the potential energy of each of the molecular orbitals, and evaluates the potential energy of the molecule itself, along with the zero-point energy, the enthalpy, Gibbs free energy, and the entropy terms.

These results allowed the calculation of the thermodynamic data of interest, as mentioned in chapter one, and tabulated it, using Microsoft Excel. After applying the thermodynamic equations eq [9-12] the following results were obtained **Table** 5.

Table 5

Theoretical quantum calculations' results for each of the studied fragments of levofloxacin, at 298K, 400K, 700K

Levofloxacin						
Fragment	**Fragment 1 (C13-N2)**			**Fragment 2 (C18-N3)**		
ΔH(0K)	383.3			323.7		
Temp.	**298K**	**400K**	**700K**	**298K**	**400K**	**700K**
ΔH (kJ/mol)	384.8	384.8	382.3	328.9	371.3	549.2
ΔS($J.K^{-1}.mol^{-1}$)	454.8	454.8	557.2	382.7	512.3	1014.5
ΔG(kJ/mol)	249.2	249.2	-7.8	214.8	166.4	-160.9
Fragment	**Fragment 3 (C4-C6)**			**Fragment 4 (C12-F)**		
ΔH(0K)	438.9			506.5		
Temp.	**298K**	**400K**	**700K**	**298K**	**400K**	**700K**
ΔH (kJ/mol)	441.5	482.8	839.5	505.3	546.2	721.4
ΔS($J.K^{-1}.mol^{-1}$)	503.7	634.3	1140.3	506.2	612.5	1045.0
ΔG(kJ/mol)	291.4	229.1	41.3	354.5	301.2	-10.0
Fragment	**Fragment 5 (C7-C9)**					
ΔH(0K)	337.7					
Temp.	**298K**	**400K**	**700K**			
ΔH (kJ/mol)	347.1	391.3	573.9			
ΔS($J.K^{-1}.mol^{-1}$)	406.7	541.2	1058.8			
ΔG(kJ/mol)	225.8	174.8	-167.2			

As these molecules that were built through the model did not contain water, it is obvious that the molecule behaves differently than the experimental behavior with respect to the reaction mechanism. This goes to prove the idea that both heterogeneity of the reaction system, and polymorphism, are key factors in the complexity of the molecule's interaction, as mentioned by previous researchers in the field (13, 14).

All results of ΔH for all the reactions at hand are highly endothermic as seen per Table 5, this means that there needed to be energy input into the system for these fragments to be dissociated. This is intuitive as these reactions are bonds breaking, and energy is always consumed during this type of change. This will be discussed further in Chapter 4.

All results of ΔG at 298K and 400K are highly endergonic as seen per Table 5, this means that the reactions are non-spontaneous at these temperatures. However, at 700K it is revealed that ΔG drops significantly and the reaction becomes spontaneous in all cases except F3. With F2 and F5 showing the lowest ΔG values, meaning these would be the most-likely bonds to dissociate spontaneously. This explains why the molecule did not start dissociation below 240 °C as seen from TGA Figure 8 and DSC results Figure B.3 in Appendix B. This will be discussed further in Chapter 4.

Figure B.4 in Appendix B and Table5 show that fragment 2 has the lowest ΔH and ΔG values at 298 K followed closely by fragment 5 and then, after an interval, fragment 1 respectively. Then at 700 K these fragments show negative ΔG values indicating their spontaneous dissociation at that temperature.

From this it is plausible to assume the most likely fragments to be separated would be at Fragment 2 and Fragment 5 nearly simultaneously, for having the lowest energy requirement as well as having consistent increments of decrease over the different temperatures. Their closeness in value hints at the possibility of both of these bonds being broken at the same time.

A close third would be fragment 1 as it shows negative ΔG value at higher temperature with lower ΔH values than the other fragments (at F3 and F4).

All primary results showed promise, precision, and reliability for further analysis, correlation to experimental analysis. This is discussed further in Chapter 4.

Chapter Four

Discussions and Conclusions

This study provided an understanding of the changes that occur on levofloxacin drug in accordance to temperature, and its decomposition products. The usefulness of these products may align with efforts to develop an effective and efficient technique for treating this pharmaceutical drug out of wastewater.

4.1 Experimental thermochemical analysis, using isoconversional methods

The experimental data in Figure 7 shows that there are two distinct mass losses that take place throughout the degradation, corresponding to the step-wise degradation of the drug. The first of which is a mass loss that appears at temperatures 235-312 °C and is confirmed by the DSC result Figure B.3 at the second peak shown from 235.5-241.5 °C which corresponds to the beginning of decomposition, with its small shouldering peak indicating the melting slightly prior to the decomposition. The second mass loss of the graph was after 350 °C, this is reaffirmed by the third peak of the DSC at 348.6 °C which shows some energy release by the molecule unlike the other two DSC Peaks, indicating bond formation, which leads to the conclusion that, at the end of decomposition, gaseous molecules such as CO_2, HF, CH_4, or NH_3 may have been formed. The formation of these molecules would indicate they are more stable than the fragments they were produced from which pushed the reaction toward their formation.

Some phantom mass measurements were observed at the higher end of the temperature scaling. These discrepancies are likely a result of the higher pressure exerted by rapid gas formation on the very sensitive mass balance (scale) of the TGA device. This is more evident as the main molecules likely to be produced during thermal decomposition under N_2 should be $\bullet CH_3$ radicals, because of the low concentrations of O_2 available. However, when O_2 is present in the reaction environment from the air these radicals would react rapidly to form CO_2 in higher quantities increasing the both the temperature and pressure in the process. That may be the reason for the American National Library of Medicine assuming the drug to be combustible (11).

These conditions and the complexity and heterogeneity of the reaction components, have proven the effectiveness of the isoconversional method for describing such solid/gas heterogenous interactions.

The effective E_α of the experiments under N_2 were calculated using the Friedman and KAS methods and it was obtained in the range 48.33 – 117.52 kJ/mol for the Friedman method. And between 23.31 – 68.47 kJ/mol for the KAS method, and increase with α.

For these data sets there was no oxygen added for many oxidation reactions to take place, while the peaks in DSC Figure B.3 show no exothermic peaks below 340 °C, with affirmation from the results of Nisar et al. (20) of E_α at 118.05 kJ/mol, leads to the conclusion that the Friedman results are more practical and indicative than their KAS counterparts.

4.2 Mass loss evaluation

To find the bond that dissociates first the mass loss ratio is evaluated at the beginning of the decomposition, and that is compared with the ratio of a fragment of the whole compound to the compound as a whole, and from Figure 7 it was noticed that the decomposition of levofloxacin starts at 235 °C, which as equation [1] indicates is a mass loss of around 4%. The molar mass of levofloxacin is 361.372 g/mol, and that of a $\bullet CH_3$ radical is 15.035 g/mol. Herein giving way to the assumption that either fragment 2 or 5 from Table 2 are the ones to dissociate first. However, the mass loss does not stagnate at that mass loss but the molecule continues to rapidly lose mass within the same temperature interval between 235-312 °C. This indicates the continuous loss of other molecules within the temperature range of 235-312 °C. And at the peak of the DTG at 312 °C, the mass loss is nearly 35% this leads to the deduction that fragments 1,2, and 5 are the ones to dissociate and in rapid succession.

4.3 Theoretical quantum calculations

The measurements from Table 5 show that the lowest bond dissociation energy amongst the bonds broken was for the at fragment 2 (C^{18}-N^3) and fragment 5 (C^7-C^9) as seen in Figure 5 and Appendix A, which confirms the experimental results of mass loss. These results together with the $\Delta G_{\text{activation}}$ value being highly endergonic, meaning the dissociation of this bond is non-spontaneous at 298 K and 400 K. However, at 700 K it is

evident that fragments F2, F5 and F1 all exhibit negative ΔG values, meaning their spontaneous dissociation is possible at high temperatures.

The values of ΔH in all five cases have been endothermic, meaning the molecules consumed energy, and that is consistent with the reactions being bond-breaking reactions, as the separation of bonds requires energy input to separate the bonding. This does not, however, rule out the possibility of net-zero output of energy whenever the radicals produced react to form other bonds. And this in turn explains the two endothermic peaks of the DSC and also explains why the exothermic peak was far to the end of the graph at higher temperature.

The values of ΔG were endergonic for all the reactions at 298 K and 400 K, meaning the threshold of activation for these reactions drops at higher temperatures, and this explains why the decomposition did not take place before 230 °C in correlation with the experimental results.

These ΔH and ΔG and entropy values, along with the experimental data, suggest the production of 2 •CH_3 radicals and that these molecules with sufficient oxygen presence are able to react and produce CO_2 gas and water molecules and give off energy in the process, and this provides some of the energy required for the bonds breaking as the decomposition carries on.

In their book on bond dissociation energies, Yu-Ran Luo (55) did not specify this bond between a methyl group and a piperazine group. However, the book mentioned the bonds shown in Table 6:

Table 6

Examples of bond dissociation energies from literature. Yu-Ran Luo. Yu-Ran Luo - Comprehensive Handbook of Chemical Bond Energies-CRC Press (2007) (55).

Bond	Energy (kJ/mol)
Trimethylamine: CH_3–$N(CH_3)_2$	315.9 ±10.5
1,1-Dimethylhydrazine: CH_3–$N(CH_3)NH_2$	377
1-Methylpyrrile: CH_3–pyrrol-1-yl	340.2 ±8.4

These results are significantly higher than the experimental and computational results obtained in this work. One reason for this is that the bonds available in the book are not of exact correspondence to the bond of interest in this work. Another reason is due to the fact that the energy is not isolated to one bond, but in fact other bonds are being stretched, broken and formed at the same time, and some of the energy granted from forming other bonds contributes to the dissociation of the bond/s of interest.

Another reason is the probability of polymorphism within the sample formation. This also explains the change in activation energy at different stages of the molecule decomposition. Where the later stages, at higher temperatures, indicate the breaking of bonds with higher energies.

All of these observations lead to the conclusion that the pyrolysis of this compound does not halt at a certain molecule but rather continues until gaseous compounds are formed such as CO_2 as per the mechanism mentioned before.

4.4 Conclusion

This research examined the thermal decomposition behavior of levofloxacin, an antibiotic drug, as a representative pharmaceutical pollutant. The investigation involved the decomposition reaction under N_2 gas environment using a TGA at various heating rates. The results of which underwent the isoconversional methods of KAS and Friedman. From these isoconversional methods, the Eα of levofloxacin's decomposition reaction was found to be between 23.3 – 68.5 kJ/mol for the KAS method, and between 48.3 – 117.5 kJ/mol for the Friedman method, increasing as a function of α.

Moreover, DSC was utilized to evaluate the heat transfer occurring as a function of temperature. The resulting data confirmed that three critical changes occur. The first of which is the dehydration of the levofloxacin hemihydrate mixture at around 100 °C. Then at around 235-312 °C the decomposition is evident occurring within a few degrees of the reported melting point of 227 °C (51). While the last DSC peak seen in the analysis results indicated bond formation after 350 °C, meaning the creation of stable molecules from the dissociation reaction products.

Furthermore, DFT calculations were used to determine the BDEs associated with each of the possible decomposition pathways of levofloxacin. DFT computational results showed

two dissociations of negative ΔG values and very close ΔH values as seen in Table 5, at the aforementioned sites of F2 and F5 from Figure 5, each dissociation producing a •CH_3 radical. The negative ΔG values indicate the spontaneity of these dissociations, while their low ΔH values indicate that these dissociations are more likely than other candidates to occur.

The overall result of DFT analysis, DSC findings, and the outcomes from the Friedman method indicated that the primary dissociation pathway is expected at the aromatic-methyl bond, yielding •CH_3 radicals. Where those radicals will then combine with available atoms to create stable gaseous molecules as a final outcome. Additionally, this combined analysis demonstrated the superior accuracy of the Friedman method over the KAS method in estimating the E_α.

4.5 Recommendations for future ventures in this field

This work focused on analyzing the thermodynamics of levofloxacin. This work is in continuation of the efforts by Badran et al. on pharmaceutical waste upgrading. Continuation into this field should aim to find more materials of similar compatibility, investigate both chemical and engineering methods to actualize this into systems of industrial operation, and study the feasibility of commercializing this process (4, 17, 21, 9, 47). Therefore, this work makes it possible to find suitable nanosorbcats that can bind and then dissociate this molecule.

This work on the kinetics of levofloxacin sheds new light on previously conducted research into the interactions it may have with other molecules, and it is imperative to reconsider, review and analyze the drug's interaction with solvents, drugs and other compounds in light of the data that this work provides, to better understand its biochemical activity and mechanism and potential risk within the medial field (20).

This study, mainly under inert circumstances (N_2) atmosphere, has noted the changes that occur via thermal decomposition. However, the study of, specifically, this molecule's combustion process may lead to further findings that may or may not assist the upgrading process's parameter-setting.

The DSC results of this work have shown a wide exothermic peak at high temperatures, for this, characterization of this peak through FT-IR may be a good qualitative tool for finding the exact composition of the products at that temperature.

This work has focused on the quantum computation with relation to the anhydrous form of the drug. Further understanding of the molecule's behavior may include a quantum computation study of the hemihydrate and monohydrate form, along with the polymorphed counterparts of the crystalline material as mentioned in previous literature (13, 14).

List of Abbreviations

Abbreviation	Meaning
TGA	Thermo-Gravimetric Analysis
KAS	Kissinger–Akahira–Sunose
E_α	Effective activation energy
α	Extent Of the Reactant Conversion
DSC	Differential Scanning Calorimetry
DFT	Density Functional Theory
BDE	Bond Dissociation Energy
PPCP	Pharmaceutical and Personal Care Product
WWTP	Wastewater Treatment Plant
DNA	Deoxyribonucleic Acid
DDD	Defined Daily Dose
Δm	Current Mass Change
Δm_{tot}	Total Mass Change
eq	Equation
t	Time
T	Temperature
k(T)	Rate Constant
A	Preexponential Factor
R	Normal Gas Constant
ΔT	Temperature Range
β	Heating Rate
i	Identity Of the Temprature Program
OFW	Ozawa-Flynn-Wall

Abbreviation	Meaning
ΔG	Change in Gibbs free energy
ΔS	Change in Entropy
SPE	Single Point Energy
ZPE	Zero Point Energy
$H_{corr.}$	Thermal Correction to Enthalpy
$S_{corr.}$	Correction to Entropy
ΔH	Change in Enthalpy
WTE	Waste-To-Energy
IUPAC	The International Union of Pure and Applied Chemistry
g/mol	Grams per mole
RSD	Relative Standard Deviation
DTG	Rate Of Change of Mass with Respect to Temperature
°C	Degrees Celsius/ Degrees Centigrade
K	Kelvin
kJ/mol	Kilo Joules per mole
R^2	Square Coefficient of determination

References

1. Harris DC. Quantitative chemical analysis. 8th ed. New York: W.H. Freeman and Co; 2010.

2. Vyazovkin S. Isoconversional Kinetics of Thermally Stimulated Processes. Cham: Springer International Publishing; 2015.

3. Peter Atkins Julio De Paula. ATKINS' PHYSICAL CHEMISTRY. Eighth Edition. Oxford University Press; 2006. (Library of Congress Control Number: 2005936591).

4. Badran I, Hassan A, Manasrah AD, Nassar NN. Experimental and theoretical studies on the thermal decomposition of metformin. J Therm Anal Calorim 2019; 138(1):433–41.

5. Kibuye FA, Gall HE, Elkin KR, Ayers B, Veith TL, Miller M et al. Fate of pharmaceuticals in a spray-irrigation system: From wastewater to groundwater. Sci Total Environ 2019; 654:197–208.

6. Couto CF, Lange LC, Amaral MC. Occurrence, fate and removal of pharmaceutically active compounds (PhACs) in water and wastewater treatment plants—A review. Journal of Water Process Engineering 2019; 32:100927.

7. Amit K. Thakur, Rahul Kumar, Ashutosh Kumar, Ravi Shankar, Nadeem A. Khan, Kaushal Naresh Gupta, Mahendra Ram, Raj Kumar Arya. Pharmaceutical waste-water treatment via advanced oxidation based integrated processes: An engineering and economic perspective .Journal of Water Process Engineering 2023; 54. Available from: URL: https://doi.org/10.1016/j.jwpe.2023.103977.

8. Wang J, Wang S. Removal of pharmaceuticals and personal care products (PPCPs) from wastewater: A review. J Environ Manage 2016; 182:620–40.

9. Riyaz NS, Badran I. The catalytic thermo-oxidative decomposition of glimepiride using the isoconversional method. J Therm Anal Calorim 2022; 147(19):10755–65.

10. Ebele AJ, Abou-Elwafa Abdallah M, Harrad S. Pharmaceuticals and personal care products (PPCPs) in the freshwater aquatic environment. Emerging Contaminants 2017; 3(1):1–16.

11. Vivek Podder, Nazia M. Sadiq. Levofloxacin: National Library of Medicine; 2022 [cited 2023 Sep 21]. Available from: URL: https://www.ncbi.nlm.nih.gov/books/NBK545180/#:~:text=Levofloxacin%20is%20FDA-approved%20for,skin%20structure%20infections%2C%20prophylaxis%2C%20and.

12. ORTHO-McNEIL PHARMACEUTICAL, INC. LEVAQUIN data sheet publication. U.S. FDA access data publication: U.S. FDA; 2006 [cited 2023 Sep 15].

13. Pereira RN, Fandaruff C, Riekes MK, Monti GA, Campos CEM de, Cuffini SL et al. Grinding effect on levofloxacin hemihydrate. J Therm Anal Calorim 2015; 119(2):989–94.

14. Wei N, Jia L, Shang Z, Gong J, Wu S, Wang J et al. Polymorphism of levofloxacin: structure, properties and phase transformation. CrystEngComm 2019; 21(41):6196–207.

15. Blondeau JM. Fluoroquinolones: mechanism of action, classification, and development of resistance. Surv Ophthalmol 2004; 49 Suppl 2:S73-8.

16. Klein EY, van Boeckel TP, Martinez EM, Pant S, Gandra S, Levin SA et al. Global increase and geographic convergence in antibiotic consumption between 2000 and 2015. Proc Natl Acad Sci U S A 2018; 115(15):E3463-E3470.

17. Badran I, Manasrah AD, Hassan A, Nassar NN. Kinetic study of the thermo-oxidative decomposition of metformin by isoconversional and theoretical methods. Thermochimica Acta 2020; 694:178797.

18. Honigsbaum M. Superbugs and us. Lancet 2018; 391(10119):420.

19. Zhou Z, Zhang Z, Feng L, Zhang J, Li Y, Lu T et al. Adverse effects of levofloxacin and oxytetracycline on aquatic microbial communities. Sci Total Environ 2020; 734:139499.

20. Nisar J, Iqbal M, Iqbal M, Shah A, Akhter MS, Sirajuddin et al. Decomposition Kinetics of Levofloxacin: Drug-Excipient Interaction. Zeitschrift für Physikalische Chemie 2020; 234(1):117–28.

21. Badran I, Manasrah AD, Nassar NN. A combined experimental and density functional theory study of metformin oxy-cracking for pharmaceutical wastewater treatment. RSC Adv 2019; 9(24):13403–13.

22. Menczel JD, Prime RB. Thermal analysis of polymers: Fundamentals and applications. Hoboken N.J.: John Wiley; 2009.

23. Saadatkhah N, Carillo Garcia A, Ackermann S, Leclerc P, Latifi M, Samih S et al. Experimental methods in chemical engineering: Thermogravimetric analysis—TGA. Can J Chem Eng 2020; 98(1):34–43.

24. Fatemeh Zamani-Babgohari, Ahmad Irannejad, Gholam Reza Khayati, Maryam Kalantari. Non-isothermal decomposition kinetics of commercial polyacrylamide hydrogel using TGA and DSC techniques. Thermochimica Acta 2023; 725(0040-6031). Available from: URL: https//:www.sciencedirect.com/science/article/pii/S0040603123001016.

25. N. Sbirrazzuoli, Y. Girault, L. Elegant. Simulations for evaluation of kinetic methods in differential scanning calorimetry.: methods and isoconversional methods Part 3 - Peak maximum evolution. Thermochimica Acta 1997; 293:25–37. Available from: URL: https://www.sciencedirect.com/science/article/abs/pii/S0040603197000233?via%3Dihub.

26. Khawam A, Flanagan DR. Role of isoconversional methods in varying activation energies of solid-state kinetics. Thermochimica Acta 2005; 429(1):93–102.

27. El-Qanni A, Nassar NN, Vitale G, Hassan A. Maghemite nanosorbcats for methylene blue adsorption and subsequent catalytic thermo-oxidative decomposition: Computational modeling and thermodynamics studies. J Colloid Interface Sci 2016; 461:396–408.

28. U.S.- EPA. Energy Recovery from Waste: Wastes - Non-Hazardous Waste - Municipal Solid Waste; 2016 [cited 2023 Sep 23]. Available from: URL: https://archive.epa.gov/epawaste/nonhaz/municipal/web/html/index-11.html#:~:text=Energy%20recovery%20from%20waste%20is,to-energy%20(WTE).

29. .Welfle A, Alawadhi A. Bioenergy opportunities, barriers and challenges in the Arabian Peninsula – Resource modelling, surveys & interviews. Biomass and Bioenergy 2021; 150:106083.

30. Neese F. The ORCA program system. WIREs Comput Mol Sci 2012; 2(1):73–8.

31. Neese F. Software update: the ORCA program system, version 4.0. WIREs Comput Mol Sci 2018; 8.(1)

32. Neese F. Software update: The ORCA program system—Version 5.0. WIREs Comput Mol Sci 2022; 12.(5)

33. Neese F, Wennmohs F, Becker U, Riplinger C. The ORCA quantum chemistry program package. J Chem Phys 2020; 152(22):224108.

34. Petrenko T, DeBeer George S, Aliaga-Alcalde N, Bill E, Mienert B, Xiao Y et al. Characterization of a genuine iron(V)-nitrido species by nuclear resonant vibrational spectroscopy coupled to density functional calculations. J Am Chem Soc 2007; 129(36):1105.60–3

35. Petrenko T, Sturhahn W, Neese F. First-principles calculation of nuclear resonance vibrational spectra. Hyperfine Interact 2007; 175(1-3):165–74.

36. Terpugova S, Degtyareva O, Savransky V, Terpugov E. Light-Induced Mid-Infrared Emission of Liquid Carbon Tetrachloride and Benzene. AJAC 2015; 06(09):731–45.

37. Grimme S. Supramolecular binding thermodynamics by dispersion-corrected density functional theory. Chemistry 2012; 18(32):9955–64.

38. Grimme S, Antony J, Ehrlich S, Krieg H. A consistent and accurate ab initio parametrization of density functional dispersion correction (DFT-D) for the 94 elements H-Pu. J Chem Phys 2010; 132(15):154104.

39. Grimme S, Hansen A. A practicable real-space measure and visualization of static electron-correlation effects. Angew Chem Int Ed Engl 2015; 54(42):12308–13.

40. Gilson MK, Irikura KK. Symmetry numbers for rigid, flexible, and fluxional molecules: theory and applications. J Phys Chem B 2010; 114(49):16304–17.

41. Gilson MK, Irikura KK. Symmetry numbers for rigid, flexible, and fluxional molecules: theory and applications. J Phys Chem B 2010; 114(49):16304–17.

42. Parr, R. G., & Yang, W. Density-functional theory of atoms and molecules. Oxford University Press; 1989.

43. Cramer CJ. Essentials of computational chemistry: Theories and models. 2nd ed. Chichester West Sussex England, Hoboken NJ: Wiley; 2004.

44. Engel E, Dreizler RM. Density Functional Theory. Berlin, Heidelberg: Springer Berlin Heidelberg; 2011.

45. Badran I, Sahar Riyaz N, Shraim AM, Nassar NN. Density functional theory study on the catalytic dehydrogenation of methane on MoO3 (0 1 0) surface. Computational and Theoretical Chemistry 2022; 1211:113689.

46. Weigend F, Ahlrichs R. Balanced basis sets of split valence, triple zeta valence and quadruple zeta valence quality for H to Rn: Design and assessment of accuracy. Phys Chem Chem Phys 2005; 7(18):3297–305.

47. Badran I, Rauk A, Shi YJ. Theoretical study on the ring-opening of 1,3-disilacyclobutane and H2 elimination. J Phys Chem A 2012; 116(48):11806–16.

48. I. Badran, K. Hashlamoun, N. N. Nassar. Bond dissociation energies of the fifth-row elements (In□I): A quantum theoretical benchmark study. Int. J. Quantum Chem. 2023; 123(23). Available from: URL: https://doi.org/10.1002/qua.27222.

49. Ding L, Zheng W, Wang Y. Theoretical study on homolytic C(sp 2)–O cleavage in ethers and phenols. New J. Chem. 2015; 39(9):6935–43.

50. Prohaska T, Irrgeher J, Benefield J, Böhlke JK, Chesson LA, Coplen TB et al. Standard atomic weights of the elements 2021 (IUPAC Technical Report). Pure and Applied Chemistry 2022; 94(5):573–600.

51. O'Neil, M.J. The Merck Index: An Encyclopedia of Chemicals, Drugs, and Biologicals. Version 13. Whitehouse Station, NJ: Merck and Co., Inc.; 2001. Available from: URL: https://merckindex.rsc.org.

52. Sanaf. Sanaf TGA Device. Available from: URL: https://sanaf.com/tga./

53. Origin: Scientific Data Analysis and Graphing Software. Version 2023. OriginLab; 2023. Available from: URL: ww.OriginLab.com.

54. Avogadro: Molecular Editor and Visualization. Version 2022. open source; 2022. Available from: URL: https://avogadro.cc.

55. Yu-Ran Luo. Yu-Ran Luo - Comprehensive Handbook of Chemical Bond Energies-CRC Press.(2007)

Appendices

Appendix A

Levofloxacin fragments' structure as used for the computational side of this work

<table>
<tr><th>Fragment</th><th>Bond</th><th colspan="2">Composition</th></tr>
<tr><td rowspan="2">Levofloxacin (whole molecule)</td><td rowspan="2">-</td><td> 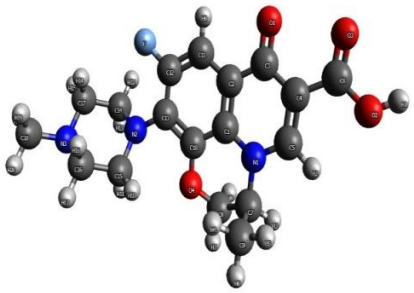 </td><td> 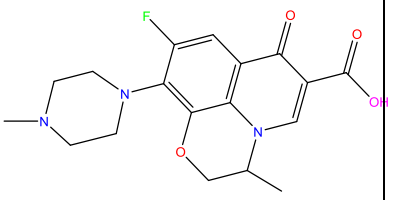 </td></tr>
<tr><td colspan="2">Molar mass = 361.372 g/mol</td></tr>
<tr><td rowspan="3">Fragment 1</td><td rowspan="3">C^{13}-N^{2}</td><td>C^{13} side</td><td>N^{2} side</td></tr>
<tr><td> 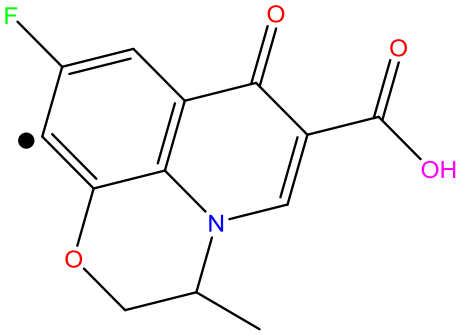
 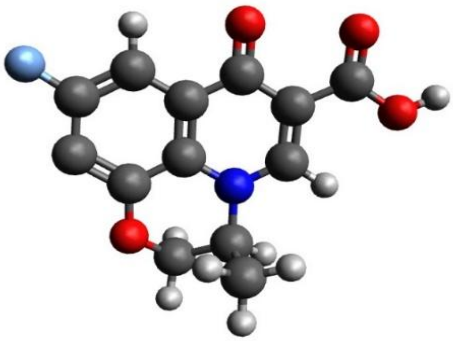 </td><td> 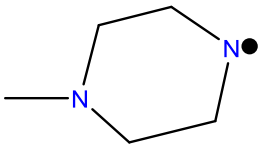
 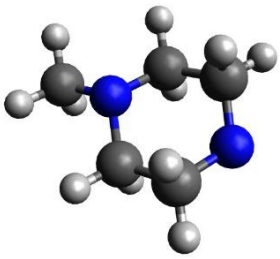 </td></tr>
<tr><td>Molar mass = 262.215g/mol</td><td>Molar mass = 99.157g/mol</td></tr>
</table>

<table>
<tr><td rowspan="2">Fragment 2</td><td rowspan="2">C^{18}-N^3</td><td>N^3 side</td><td>C^{18} side</td></tr>
<tr><td> 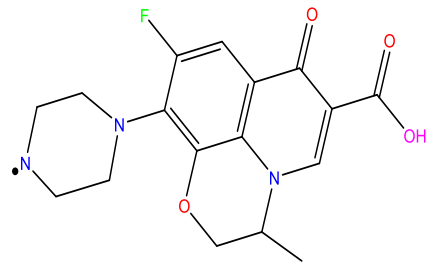

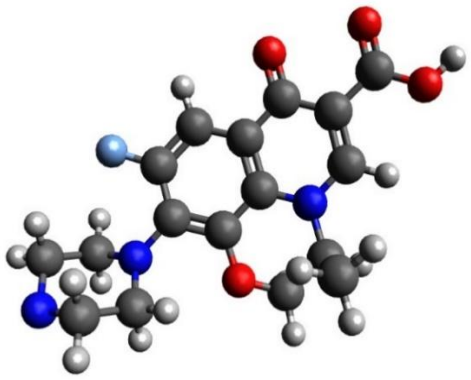
Molar mass = 346.337g/mol</td><td> 


Molar mass = 15.035g/mol</td></tr>
<tr><td rowspan="2">Fragment 3</td><td rowspan="2">C^4-C^6</td><td>C^4 side</td><td>C^6 side</td></tr>
<tr><td> 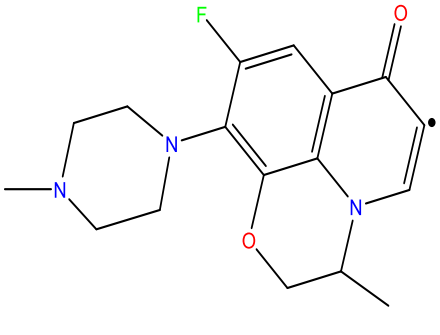

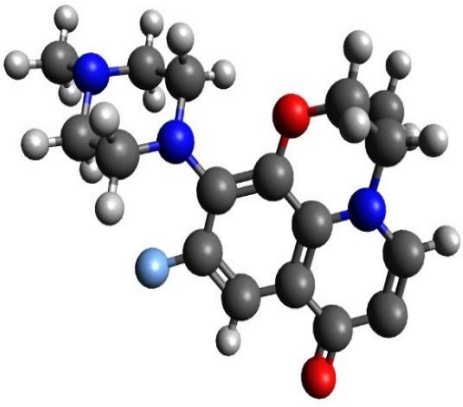
Molar mass = 316.355g/mol</td><td> 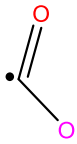

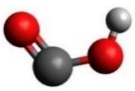
Molar mass = 45.017g/mol</td></tr>
</table>

<table>
<tr><td rowspan="2">Fragment 4</td><td rowspan="2">C^{12}-F</td><td>C^{12} side</td><td>F side</td></tr>
<tr><td> 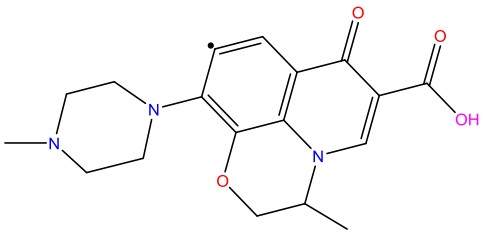

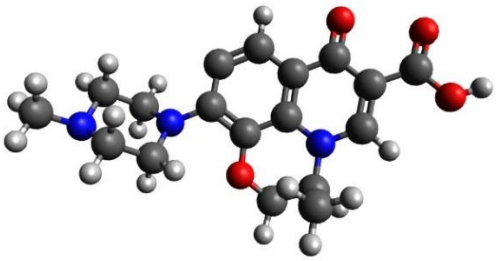
Molar mass = 342.375g/mol</td><td> 


Molar mass = 18.997g/mol</td></tr>
<tr><td rowspan="2">Fragment 5</td><td rowspan="2">C^{7}-C^{9}</td><td>C^{7} side</td><td>C^{9} side</td></tr>
<tr><td> 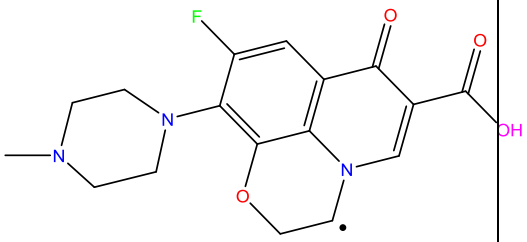

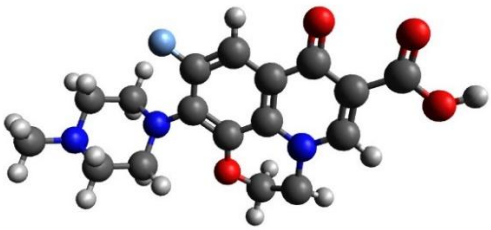
Molar mass = 346.337g/mol</td><td> 


Molar mass = 15.035g/mol</td></tr>
</table>

Appendix B

Figures

Figure B.1

Arrhenius plot of the KAS method results, with linear fitting. The R^2 value are tabulated in Table4

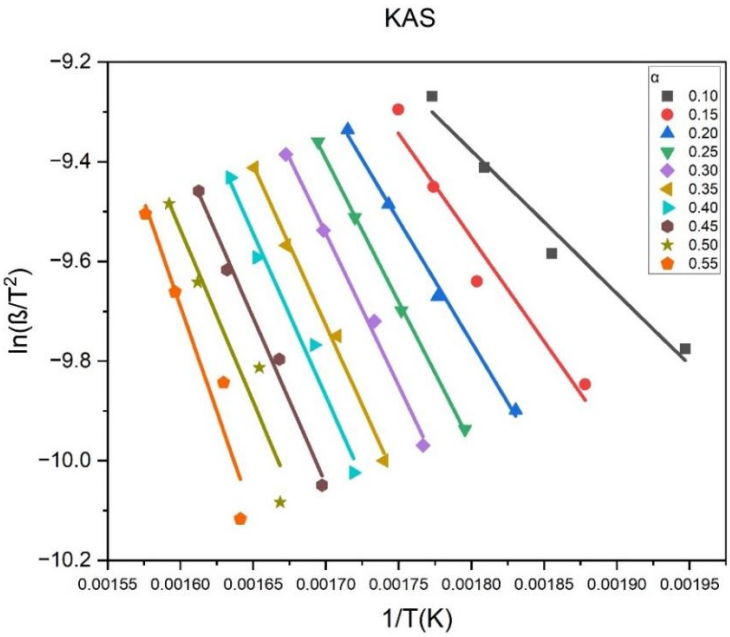

Figure B.2

E_α as a function of α for levofloxacin under N_2 gas. With error margins obtained through the RSD for each method at each point. Error bars represent the relative standard deviation measurement.

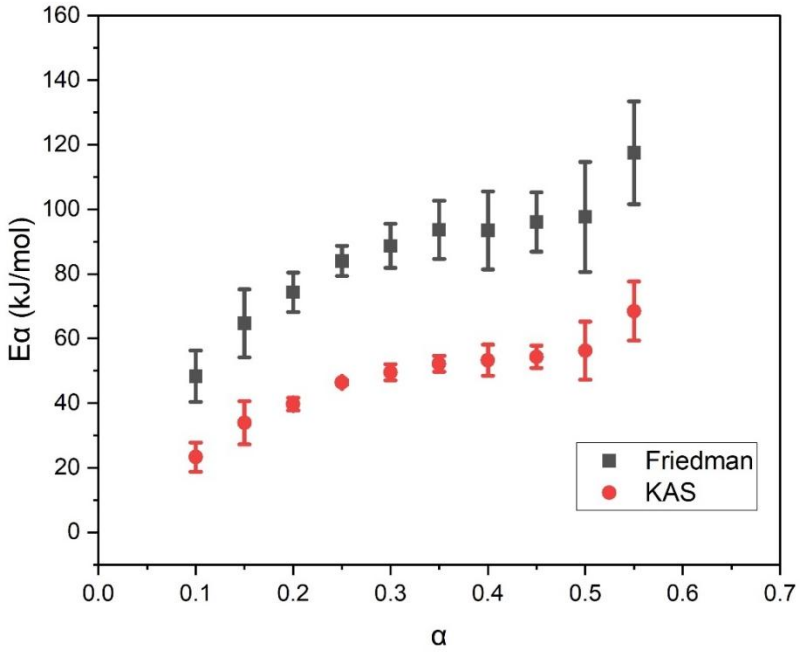

Figure B.3

DSC results for levofloxacin under N_2 gas, performed at the University of Jordan. sample of 5.422 mg of the levofloxacin hemihydrate. And the 'atmosphere' remark denotes the gaseous medium under which the experiment was conducted, which is N_2 gas at a flow rate between 20.0 ml/min and 60.0 ml/min.

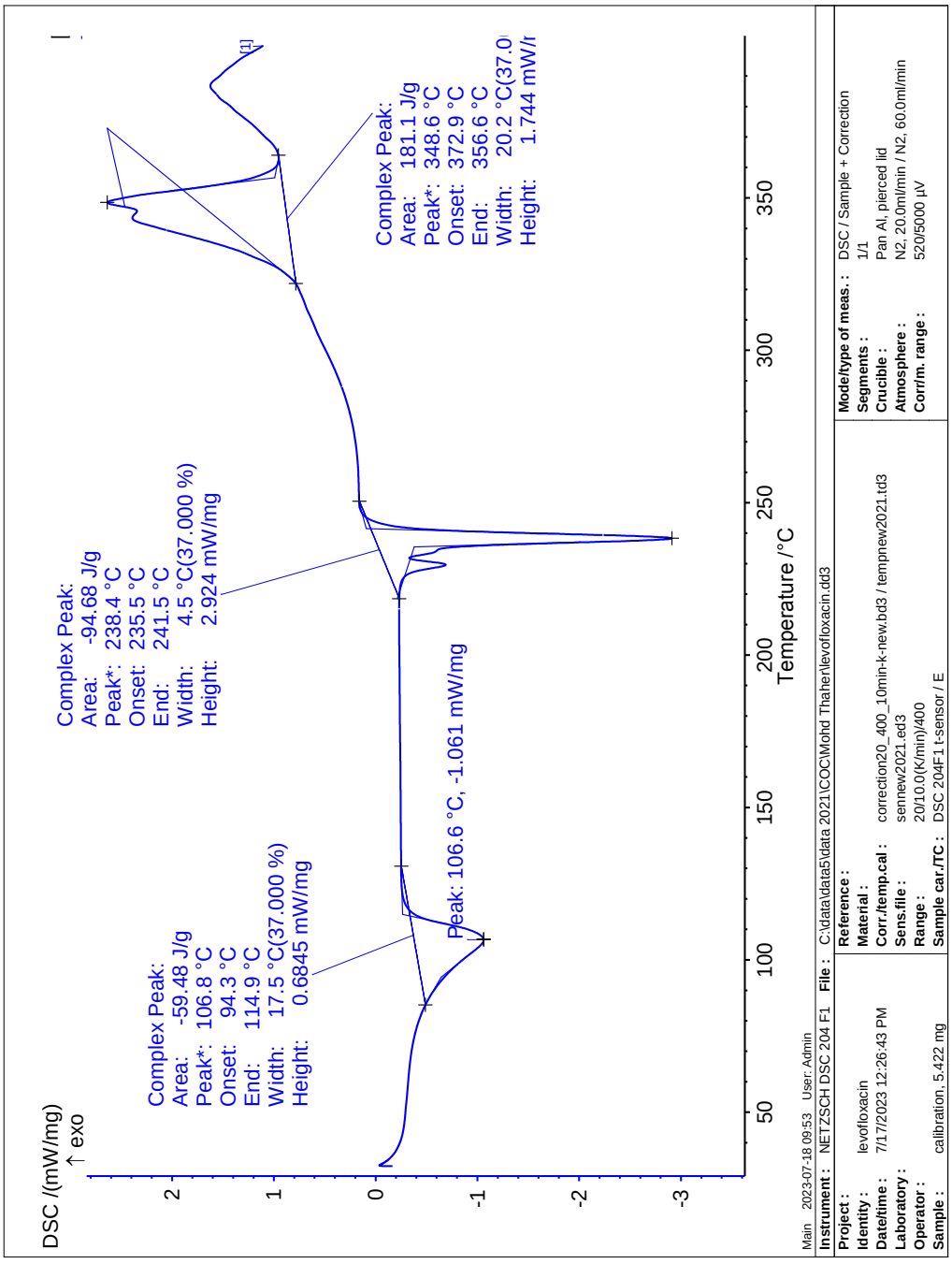

Figure B.4

Theoretical quantum calculations' results of ΔH and ΔG for each of the studied fragments of levofloxacin, at 298K

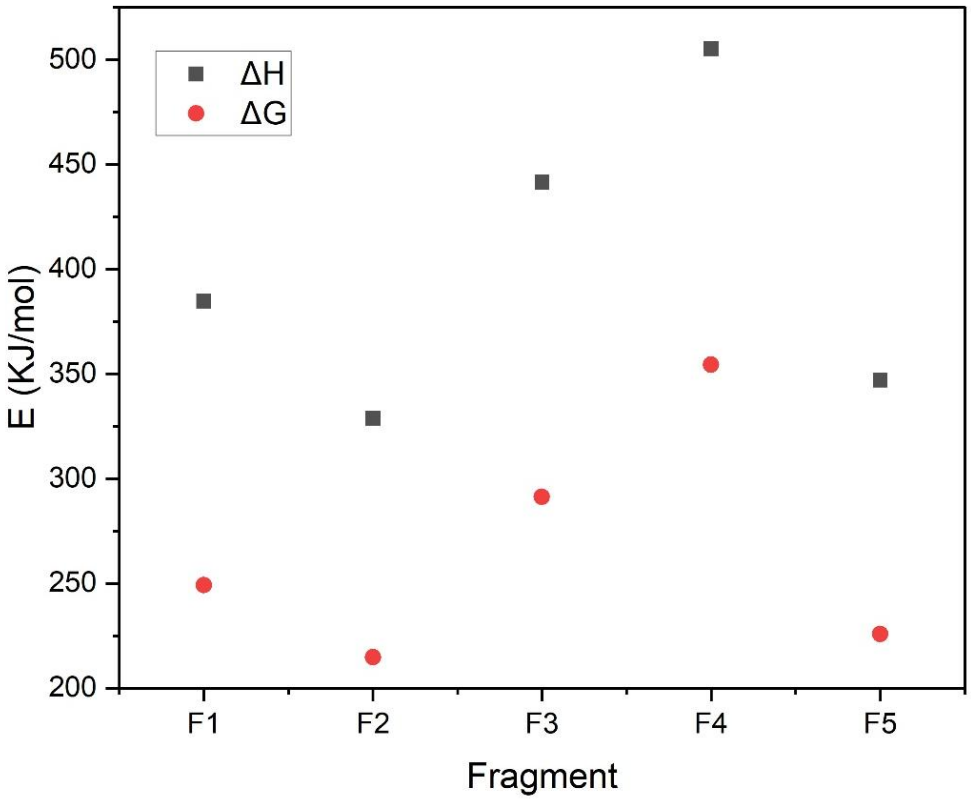

جامعة النجاح الوطنية
كلية الدراسات العليا

تحليل التحلل التأكسدي الحراري لدواء ليفوفلوكساسين بواسطة الخواص الحركية المتقاربة والطرق الحسابية الكمية المحوسبة

إعداد
"محمد نشأت" أحمد محمود ظاهر

إشراف
د. إسماعيل بدران

قدمت هذه الرسالة استكمالا لمتطلبات الحصول على درجة الماجستير في الكيمياء،
من كلية الدراسات العليا، في جامعة النجاح الوطنية، نابلس – فلسطين.

2024

تحليل التحلل التأكسدي الحراري لدواء ليفوفلوكساسين بواسطة الخواص الحركية المتقاربة والطرق الحسابية الكمية المحوسبة

إعداد

"محمد نشأت" أحمد محمود ظاهر

إشراف

د. إسماعيل بدران

الملخص

تناولت هذه الدراسة سلوك التحلل الحراري لعقار ليفوفلوكساسين، وهو دواء مضاد حيوي يمكن اعتباره مثالًا نموذجيًا للملوثات الدوائية، وقد شملت الدراسة تحليل تفاعل التحلل تحت غاز النيتروجين باستخدام جهاز التحليل الحراري الوزني TGA بمعدلات تسخين مختلفة، ثم تم تطبيق حسابات طرق التحول المتساوي KAS و Friedman على نتائج TGA، ومن خلال هذه الطرق الحسابية، تم العثور على قيمة طاقة التنشيط الفعلية E_α لتفاعل تحلل الليفوفلوكساسين بين 23.3 – 68.5 كيلو جول/مول لطريقة KAS ، وبين 48.3 – 117.5 كيلو جول/مول لطريقة Friedman، وقد تناسبت طردياً بزيادة α.

بالإضافة إلى ذلك، فقد تم استخدام المسح الحراري التفاضلي DSC لتقييم انتقال الحرارة الحاصل بدلالة درجة الحرارة، وأكدت البيانات الناتجة عن ذلك وجود ثلاث تغييرات حرجة، الأولى منها هي تجفيف مزيج الليفوفلوكساسين المائي عند حوالي 100 درجة مئوية، ثم يظهر التحلل عند حوالي 235–312 درجة مئوية، حيث يحدث على بعد بضع درجات مئوية من نقطة الانصهار والتي هي 227 درجة مئوية. بينما أشارت ذروة DSC الأخيرة المرئية في نتائج التحليل إلى تكوين روابط بعد 350 درجة مئوية، مما يعني تكوين جزيئات مستقرة من منتجات تفاعل التحلل.

علاوة على ذلك فقد تم استخدام حسابات النظرية الكثافية DFT لتحديد قيم طاقات الروابط BDEs الدالة لكل من مسارات تفكك الليفوفلوكساسين المحتملة، وأظهرت النتائج الحاسوبية للـــDFT حالتين تظهران قيم ΔG سالبة وقيمΔH متقاربةً جدًا كما هو موضح في الجدول 5، عند المواقع F2و F5 من الشكل 5، حيث ينتج كل تفاعل

تحلل جزيئ CH_3•، ذلك بأنّ القيم السالبة لـــ ΔG تشير إلى تلقائية هذه التفاعلات، في حين تشير قيم ΔH المنخفضة إلى أنّ هذه التفاعلات أكثر احتمالاً من غيرها للحدوث.

وبالتالي فقد أظهرت النتائج العامة لتحليل DFT ونتائج DSC ونتائج طريقتي KAS و Friedman أن المسار التفككي الرئيسي متوقع عند رابطة الأروماتية–الميثيلية، مما يؤدي إلى إنتاج جزيئات CH_3•، حيث ستتحد هذه الجزيئات بالذرات المتاحة لإنشاء جزيئات غازية مستقرة كنتيجة نهائية.

الكلمات المفتاحية: صيدلة؛ التحليل الوزني الحراري؛ المسح التفاضلي للسعرات الحرارية؛ التحويل المتساوي؛ الكيمياء الحاسوبية؛ الامتزاز.